

**MANUAL FOR NORFLAG, VERSION 3.0
(UPDATED VERSION OF FORMER WINFLAG 2.4**

BY

TOR ERIK VIGRAN

Trondheim 17.10.2016

CONTENTS

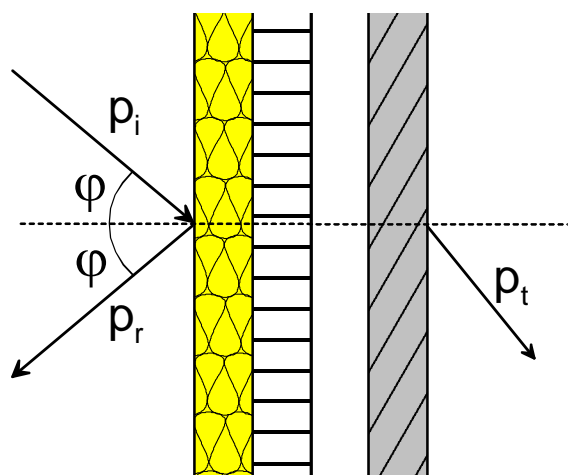
1	Introduction	4
2	Overview	5
3	Main features	5
3.1	New features (updates from WINFLAG version 2.4).....	6
4	Brief description of the program	7
4.1	Calculation options.....	8
4.2	Program execution. some examples	8
5	Menus	12
5.1	The file menu	12
5.1.1	Making a report	14
5.2	The Add Layer Menu	15
5.2.1	The air layer	18
5.2.2	Porous facing.....	19
5.2.3	Porous layers	19
5.2.3.1	Model by Allard and Johnson with a “limp” model modification.	19
5.2.3.2	Model by Attenborough	21
5.2.3.3	Model by Delany and Bazley	21
5.2.3.4	Model by Komatsu	22
5.2.3.5	Model by Mechel	22
5.2.3.6	Model by Sgard et.al. Double porosity materials	23
5.2.3.7	Model by Wilson	24
5.2.4	Slotted plate (Slatted panel)	25
5.2.4.1	Regular long slots.....	25
5.2.4.2	Regular rectangular slots	26
5.2.4.3	Conical (wedge-shaped) long slots	27
5.2.5	Perforated plate	28
5.2.5.1	Regular holes.....	28
5.2.5.2	Regular holes with fabric	29
5.2.5.3	Conical holes	29
5.2.5.4	Microperforated.....	29
5.2.6	Limp mass	30
5.2.7	Solid plate (panel)	30
5.2.7.1	Thin plate.....	31
5.2.7.2	Thick plate (elastic)	31
5.2.7.3	Corrugated plates.....	32
5.2.7.4	Sandwich	34
5.2.8	Structural bridges	35

5.2.8.1	Stiff structural bridges	36
5.2.8.2	Flexible bridges	37
5.3	The frequency menu	39
5.4	The sound incidence menu	40
5.4.1	Statistical absorption and transmission coefficients.....	40
5.4.2	Weighted sound absorption coefficient.....	41
5.4.3	Weighted sound reduction index.....	42
5.5	The sample size menu	43
5.6	The result menu	45
5.7	The diagram menu.....	46
5.8	The help menu	47
6	Attenuation in ducts (silencers).....	48
6.1	Rectangular duct with lining on two walls.....	49
6.2	Circular duct.....	50
ANNEX A.	Configuration file	52
ANNEX B.	Properties of materials	53
ANNEX C.	Measurement and calculation on a microperforated membrane.....	55
ANNEX D.	Measurements and calculations on a resonator panel using perforation with conically shaped holes.....	56
ANNEX E.	Spatial windowing in transmission loss calculations. Example: the sound reduction index of a double-leaf construction.....	57
ANNEX F.	Stiff structural connections (ties and studs) in double walls. Example: Wall with acoustical lining.....	58
ANNEX G.	Flexible structural connections in double walls. Example: Lightweight double wall with cavity infill	59
Annex H1.	Example on combining several thick (flexible) plate layers. Laminated glass with PVB (Polyvinyl butyaryl).....	60
Annex H2.	Example on combining several thick (flexible) plate layers. Multi-layered panel; steel plate, mineral wool and laminate.	61
Annex I.	Example on double porosity material. Measured and predicted results on a fibrous material.....	62

1 INTRODUCTION

The program calculates the absorption coefficient, the impedance and the sound reduction index for constructions combined of material layers of different types (porous materials, perforated plates etc.). As an add-on to the program, one may calculate the approximate sound attenuation in dB/m for lined ducts, either a rectangular duct lined on two sides or a circular duct lined with the specified layer construction.

Calculations may be performed at single frequencies or as mean values in one-third-octave bands, in both cases for a free field sound incidence as well as for a diffuse field. The program is modelling the acoustic properties of a combination of such layered materials using the transfer matrix method. Basically, each layer in the combination, assumed to be of infinite extent, is represented by a matrix giving the relationship between a set of physical variables on the input and output side of the layer. These matrices may then be combined to give the relationship between the relevant physical variables for the whole combination. Characteristic data as absorption coefficient, input impedance and transmission loss (sound reduction index) may then be calculated assuming plane wave incidence. The size and complexity of these



matrices, however, is totally dependent on the specific material in the actual layer, i.e. how many physical variables one have to use describing the wave motion in the material and then how many material parameters that are necessary to specify the material. In many cases, only two physical variables are sufficient which are the sound pressure and the particle velocity. A simple 2x2 matrix then describes the relationship between these variables on the input and the output side.

Figure 1-1 Combination of several layers (each of infinite extent)

For the description of layers such as thin plates (panels), perforated or non-perforated, two physical variables are always sufficient. The word "thin" here signify that we do not need to worry about the wave motion inside the plate itself; the wavelength is much longer than the thickness of the plate. With thicker elastic materials this simple model is no longer feasible. We shall at least need four physical variables, e.g. the particle velocity and the stress in two directions. Describing the relationship between the input and output we then need a 4x4 matrix. It may be shown, however, that if there are fluid layers on both sides of the elastic layer, this 4x4 matrix may be reduced to a simple 2x2 matrix. This is the procedure utilised in the WinFLAG program up to version 2.3 to include single elastic layers (denoted thick plates) and also sandwich elements. In the present version, however, these thick (elastic) plates may be directly coupled enabling calculation of the transmission loss of e.g. laminated glazing. As opposed to the sandwich "layer" included in the program, the face layers need not to be identical when assembling a sandwich construction from individual elastic layers.

Porous materials may also be included in a simple 2x2 matrix description if they are modelled as an equivalent fluid. Such a model is applicable to many porous materials, e.g. mineral wool type absorbents. The basic assumptions are that the material is homogeneous and isotropic, having pores filled with air embedded in an infinitely stiff matrix or skeleton. Again, if the elastic properties of this skeleton have to be taken into account a description

using two physical variables only is again not feasible. It is therefore not to be expected that the program NorFLAG gives correct results in the latter case, e.g. for many foam materials.

2 OVERVIEW

The program main files are the following:

- | | |
|------------------------|---|
| • NORFLAG.EXE | This is the main program |
| • FLAG_V30.DLL | "Dynamic Link Library" - calculation routines |
| • NORFLAG_HELP_3.0.PDF | Help file (this document) |

To get help during program execution the NORFLAG_HELP-file may be called from the Help menu of the main program. Please observe that there are several cross-references in the document, i.e. when sections and figures are referred to, clicking on the Section or Figure number will bring you to the item.

3 MAIN FEATURES

- Calculates the absorption coefficient with a choice of 23 different types of layers, including 7 different models of porous materials. The absorption coefficient may be calculated, with some exceptions, for any combination or any number of these layers limited to a total of 20 layers. A 24th type of layer, the infinitely hard wall, i.e. a rigid backing, may be included in the case of absorbers placed against a hard wall in a room.
- Absorption coefficients obtained in a standard reverberation room (the commonly used product data after ISO 354) may be estimated, as well as the weighted sound absorption coefficient α_w according to ISO 11654.
- The sound reduction index in dB (sound transmission loss) is simultaneously calculated for all combinations not including the infinitely hard wall. The weighted sound reduction index R_w (C; Ctr) according to ISO 717 Part 1 is also calculated when applying a diffuse field option and calculating results in one-third-octave band.
- To simulate structural connections in double lightweight walls, such as studs or point-like connections ("ties"), types of layers named *Structural bridges*, is introduced. These bridges may either be infinitely stiff or given a certain flexibility to simulate e.g. flexible steel studs in double-leaf walls.
- The acoustic impedance is also simultaneously calculated in all cases when an angle of sound incidence is specified.
- All data mentioned above may be calculated for a given angle of incidence or in a diffuse field. For the effect of structural connections, however, only diffuse field calculations are applicable.
- Calculations are performed at single frequencies or as mean values in one-third-octave bands. There is also an option for exporting calculated results as mean values in octave bands.
- As an add-on to the program the attenuation of noise in ducts, e.g. air-conditioning ducts, lined with the chosen layer configuration may be calculated.
- A report window in Rich Text Format (.rtf file) is implemented where specifications, tables of results and diagrams may easily be imported.
- Results, together with specifications for the combination of layers, may be exported to a plain text file (ASCII), alternatively to a Microsoft Excel file.

- A chosen combination of layers, a configuration, may be saved to a file and later imported for additional calculations. The same applies to single layers, which enables the user to build up a library of material layers.

Note Please be aware that due to the introduction of new layers having a higher number of parameters the reuse of configuration files from earlier WinFlag versions is not possible without some minor editing. Information is given in Annex A.

3.1 NEW FEATURES (UPDATES FROM WINFLAG VERSION 2.4)

New features in NorFlag version 3.0 include

- Another two simple models for a porous layer are added, namely the one by Komatsu; see the reference in Section 5.2.3.4, and one by Wilson; see the reference in Section 5.2.3.7. Additionally, the rigid frame model Allard/Johnson may be modified to a limp frame model by specifying the density of the material.
- To the models for porous materials is also added a model for a porous material with so-called meso-perforations, also called “double porosity materials”, as they made up of two interconnected networks of pores of quite different size. In practice, a porous material contains perforations, normally holes, with a characteristic size much larger than the pores in the material; i.e. a lateral dimension of centimetres. The model implemented is the one given by Sgard et al.; see the reference given in Section 5.2.3.6. A comparison of measurement results and predicted values is given in Annex I.
- A slightly improved model of a perforated plate (with circular holes), when combined with a resistance fabric, is constructed by defining a layer being a combination of a perforated plate and a layer of the type “porous facing” as outlined in Section 5.2.2; see Section 5.2.5.2.
- A general model for a perforated plate with rectangular slots is added; see Section 5.2.4.2
- When evaluating the weighted sound reduction index for the one-third-octave range 100–3150 Hz, the spectrum adaptation terms C and C_{tr} in decibels are added to the results; i.e. the statement of performance of the building element is as shown in the following example: $R_w(C; C_{tr}) = 41(0; -5)$ dB.

4 BRIEF DESCRIPTION OF THE PROGRAM

The program is started from your program menu, alternatively by clicking on the file NORFLAG.EXE or by making a shortcut to this file and start from the desktop. The following window should then appear (see *Figure 4-1*).

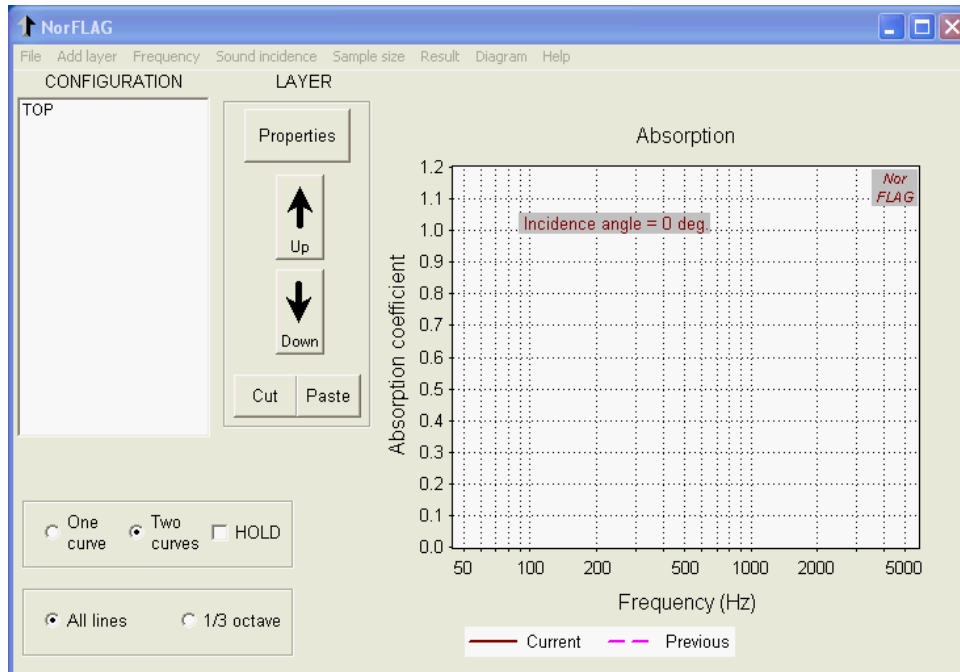


Figure 4-1. The main window at start-up time

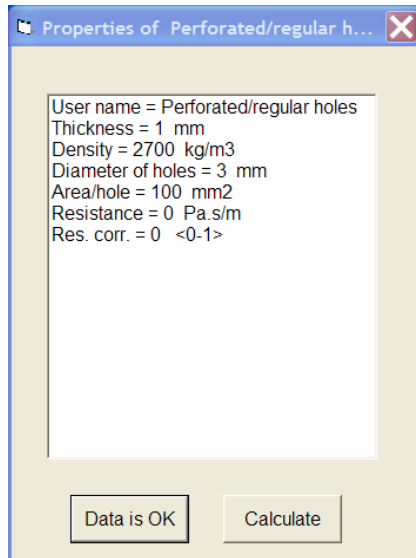
In the list box to the left (labelled CONFIGURATION and having the word TOP on the first line) one composes the combination of layers for which calculations are desired. The word TOP indicates the side of the incident plane wave in air. As mentioned in the introduction, the layers may be of the type porous materials, perforated panels etc. For a detailed description of the different types of layers, see Section 5.2 below. **Please observe that except when including the layer HARD WALL; the back of the last layer will be air (as on the incident side).**

The graphical picture to the right always shows the results of the calculations. In addition, a previous result may be displayed in the same diagram. At start up time a default diagram for the absorption coefficient is shown.

The program has, as listed below, a total of eight menus which is explained in more detail in Section 5. From the last one of these menus: **Help**, this help file may be called.

- **File** handles the configuration, layer, result and report files. Exits the program.
- **Add layer** adding a chosen type of layer (NB! no calculations are performed)
- **Frequency** frequency range of calculations, type of scale (linear, log).
- **Sound incidence** choice of angle of incidence or diffuse incidence.
- **Sample size** specifies the sample size either in the reverberation room or in the transmission suite.
- **Result** choice of calculated result (absorption, impedance, transmission and optionally duct attenuation).
- **Diagram** choice of axis scale values in the diagram.
- **Help** calling files containing either the full manual or a material property list.

To the right of the list box specifying the configuration, one will find a frame labelled **LAYER** with five command buttons. Clicking on the button **Properties** (or double-clicking in the list box) will bring up a new window giving the material properties for the layer marked in the list box. An example is shown in *Figure 4-2* where the layer is a perforated plate. Clicking on a parameter value one may change the value listed. In addition, one may exchange the default name of the layer into a chosen user name. As shown, this specification session may



be terminated by a calculation. Alternatively, the calculations may be started with the command button **Calculate** that will appear under the configuration list box. This button will appear when changes necessitate a recalculation; see the example given in *Figure 4-3*. A number of changes, however, will automatically start the calculations.

Concerning the command buttons **Up** and **Down**, shown in *Figure 4-1* or *Figure 4-3*, these will move a marked layer up or down in the configuration list box. Below these are the **Cut** and **Paste** buttons for a single layer. The layer is always pasted below a marked layer in the list.

Figure 4-2. The window listing the properties of a given layer (example Perforated plate with regular holes)

4.1 CALCULATION OPTIONS

Below the configuration list box one will find two frames containing options. The first offers the possibility of having two curves displayed; a previous result together with the current calculated result. This is the default option. Marking of the box **Hold** after a calculation will keep this result for a comparison with later results. Unmarking the box will continually update the second curve. The exception to this action is when displaying the input impedance. In this case the two curves represent the real and imaginary part of the impedance respectively, and no former results are available.

The last set of options offers the choice between calculating results for all frequency lines or mean values in one-third-octave bands, frequency range 40 Hz to 10 kHz (centre frequencies of bands). In the latter case mean values are based on a minimum of 10 frequency lines inside each one-third-octave band. In this case mean values in full octave bands are calculated as well, data that may be exported; see Note 2 below Section 5.1.

4.2 PROGRAM EXECUTION. SOME EXAMPLES

Starting the program a main calculation window will appear as shown in *Figure 4-1*. The first task for the user is to "compose" the configuration by pulling down the various layers in the configuration list box by clicking on the submenus under the menu **Add Layer**. Having done this, one may change the default parameters for each layer to the desired ones by clicking on the button **Layer properties** or double-clicking on the item in the list box. This opens up the properties window, an example of which is shown in *Figure 4-2*. When the last layer is updated one may start the calculations from this window, alternatively by the command button **Calculate** under the configuration list box, see *Figure 4-3*. A calculation will otherwise start automatically when using the menus **Frequency** or **Sound incidence**. Below

are shown examples of results from calculations of absorption coefficients, input impedance, sound reduction index and duct attenuation.

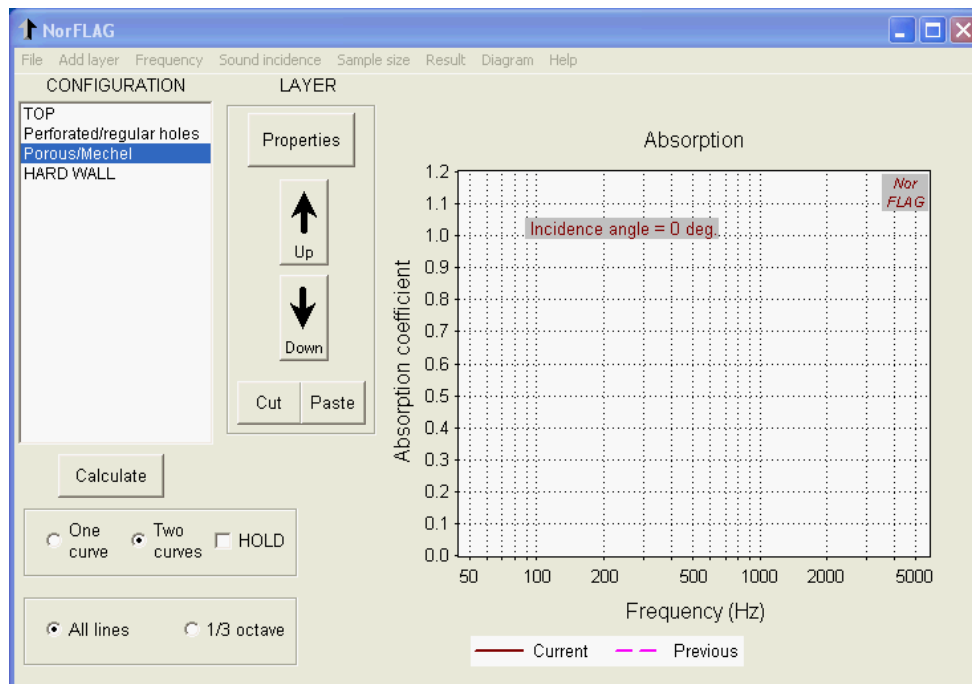


Figure 4-3. The main calculation window where layers have been entered into the configuration list box (before parameters are updated and any calculations performed)

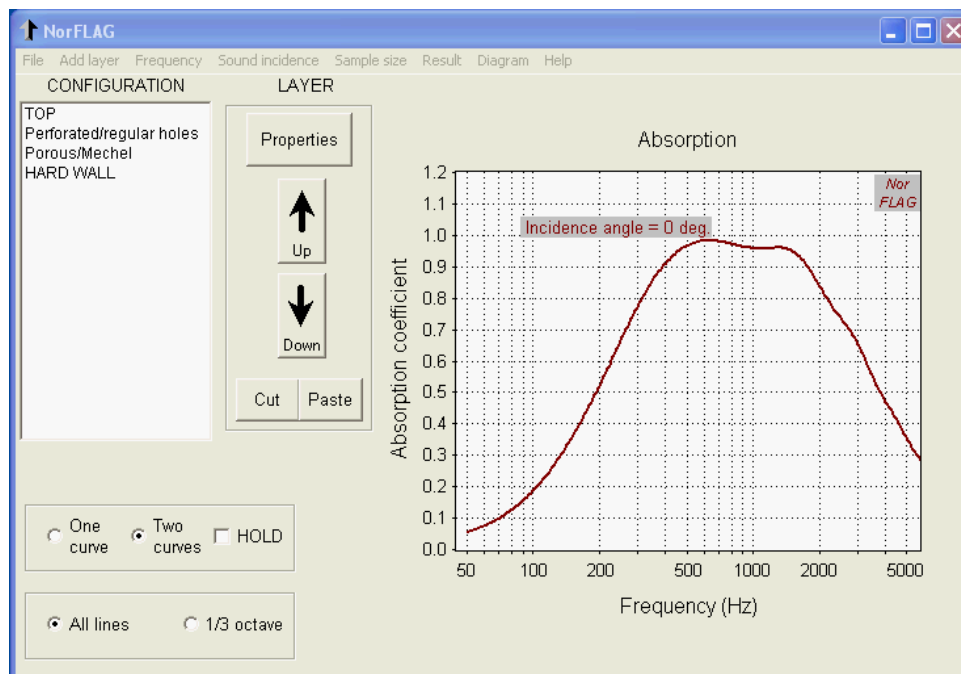


Figure 4-4. Example showing the absorption coefficient of a resonant absorber for normal incidence. The parameters for the chosen layers are the default ones except for the thickness of the porous layer (100 mm)

An example from a calculation of the absorption coefficient is shown in *Figure 4-4*. The resonant absorber is a perforated plate combined with an air space in front of a hard wall (or hard ceiling), the space filled with a porous material described using the model after Mechel. *Figure 4-5* shows the corresponding normalised input impedance for the same configuration. A more detailed description of the various models is given below under the Section 5.2.

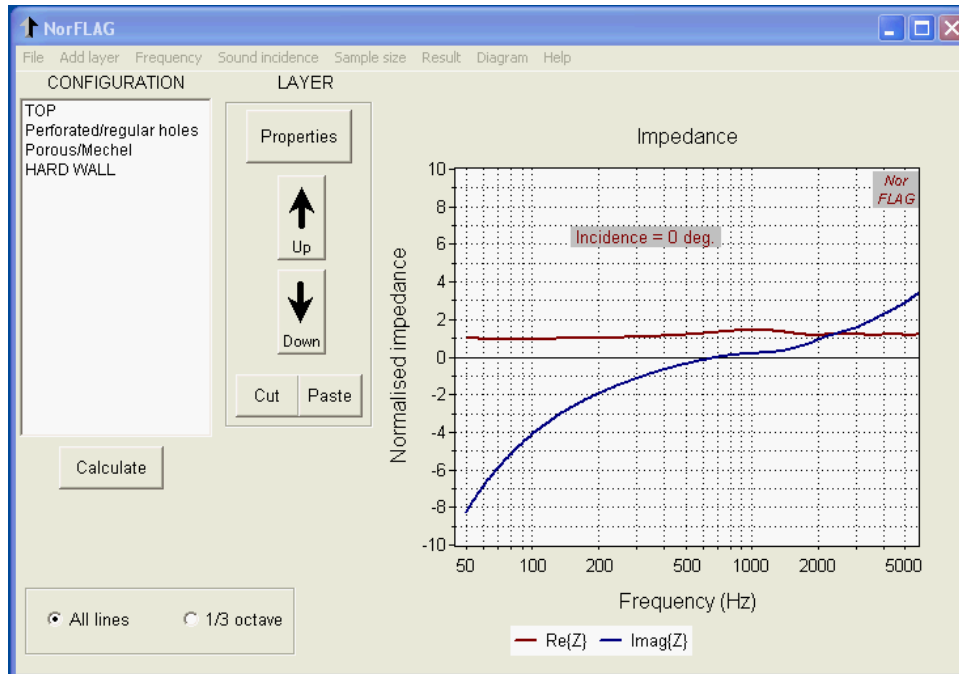


Figure 4-5. The normalised impedance corresponding to the data in Figure 4-4

Figure 4-6 shows an example of calculation of the sound reduction index of a panel or wall in a diffuse sound field. The specimen is a 250 mm aerated concrete calculated respectively as a thin plate (marked "Previous") and as thick elastic plate (marked "Current"). In contrast to the examples above, mean values in one-third-octave band are calculated. The weighted sound reduction index together with the spectral adaptation terms; i.e. $R_w(C; C_{tr})$, is given in the lower right corner.

Figure 4-7 shows an example of the calculation of sound attenuation in a lined duct of circular cross section using a lining of the same type as used in *Figure 4-4* (and *Figure 4-5*). The radius of the free air space of the duct is 150 mm. For a general description and details concerning the implementation, see Section 6. Also please see the note and illustrations in section 6.2 concerning the use of plane surface impedance for curved surfaces.

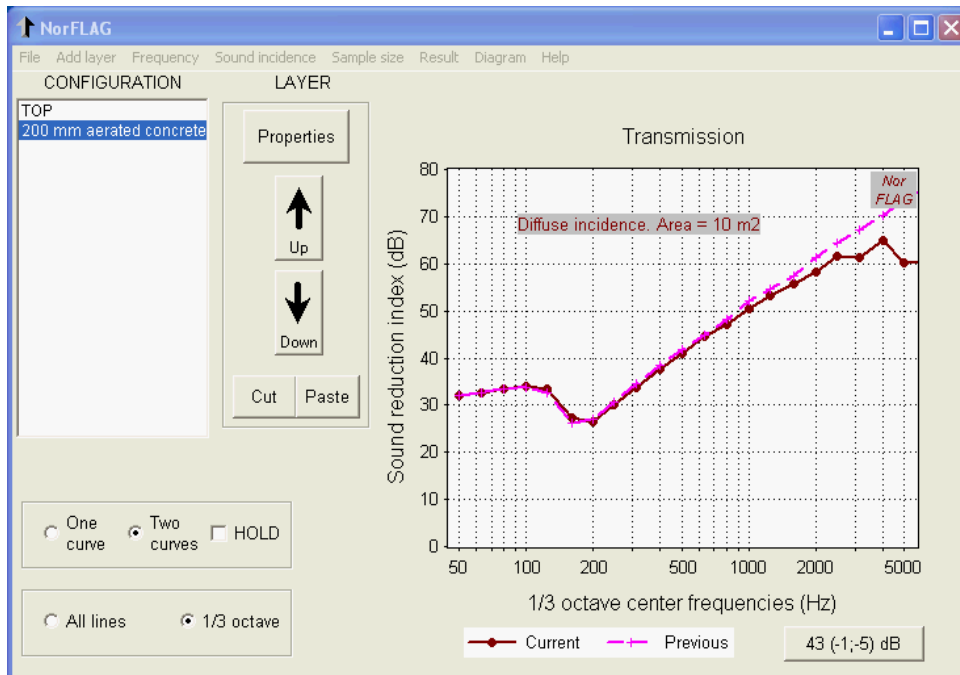


Figure 4-6 Example on the sound reduction index for a wall (aerated concrete) using layer types thin and thick plate, respectively. Diffuse sound incidence. Mean values in one-third-octave bands with weighted index and spectral adaptation terms (lower right corner).

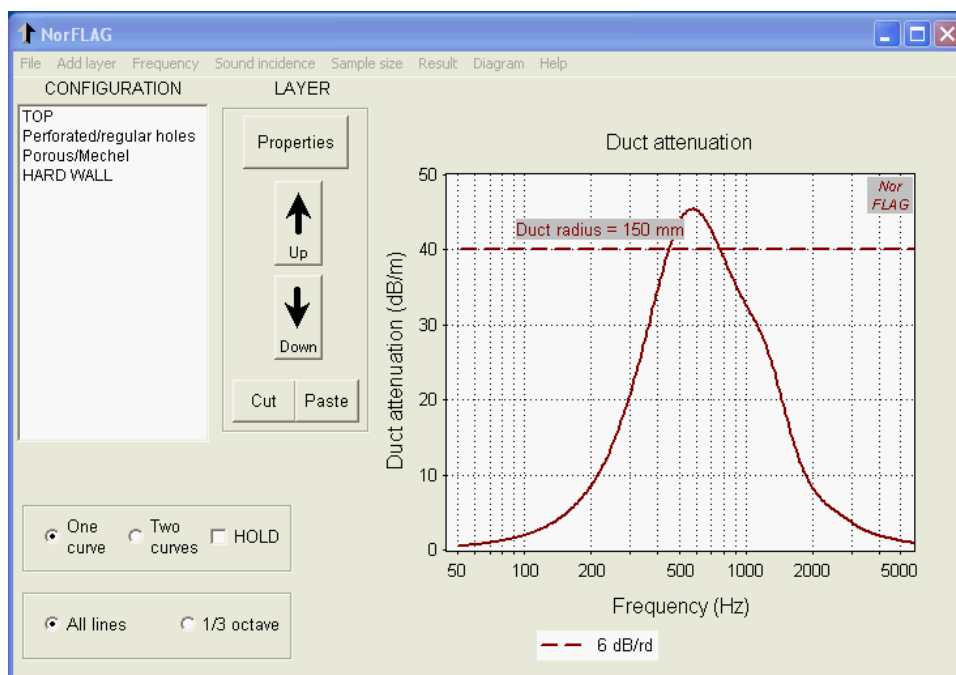


Figure 4-7. Attenuation in a lined circular duct using the resonant absorber having the impedance shown in Figure 4-5. The free air space has a radius 150 mm. The dotted line indicates a value of 6 dB per length of duct equal to the radius.

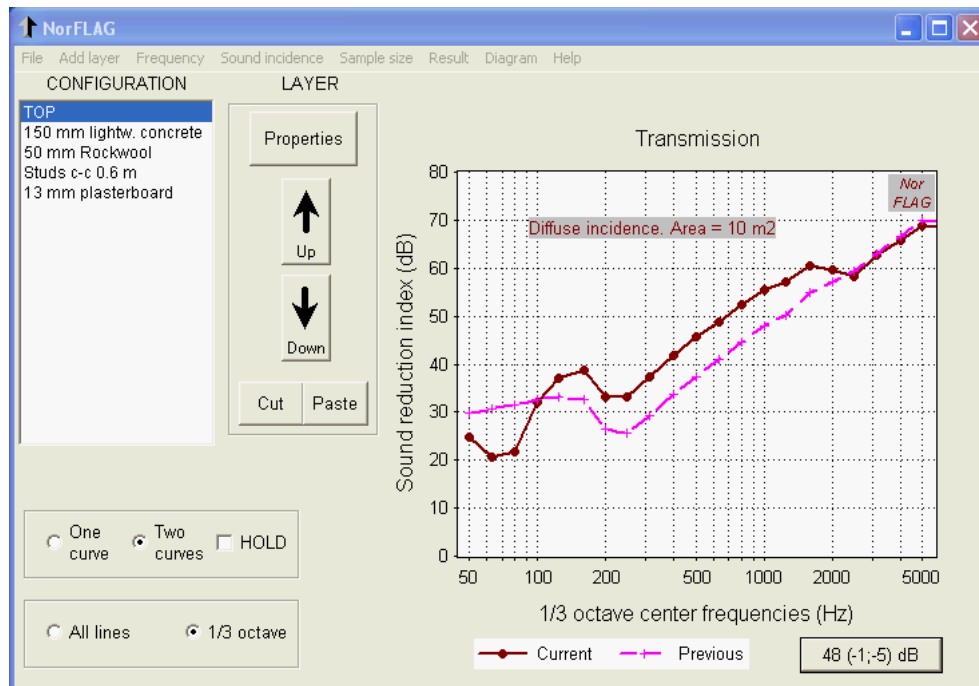


Figure 4-8 The sound transmission index of a lightweight concrete wall with an acoustical lining of 13 mm plasterboard fixed with rigid studs to the wall. The cavity is filled with mineral wool. The dashed curve shows the reduction index of the primary wall.

Finally, Figure 4-8, shows an example of the sound transmission of a double-leaf wall, applying the “layer” named *Structural bridges*, type *Stiff*. The primary wall is a lightweight concrete wall having an attached so-called acoustical lining, which is a 13 mm plasterboard mounted on studs firmly fixed to the primary wall; see also Annex F. As may be seen, the improvement due to the lining goes to zero above the coincidence frequency of the plasterboard, which is approximately 2500 Hz. Also, the double wall resonance shows up the one-third-octave band 80 Hz, giving a negative improvement.

For an example using *Structural bridges*, type *Flexible*; see Annex G.

5 MENUS

An overview of the main menus and options was given above. Below, the menus are described in more detail with explanations concerning the input data that the user must supply to the program. Specifically, this applies to the input parameters for the different layers.

5.1 THE FILE MENU

The menu contains the following submenus:

- Save configuration
- Open configuration
- Save layer data
- Export results
- Export data to NorRT60
- Make report
- Report window
- EXIT

The first four submenus will open up the Microsoft standard window for saving/opening files. The next item concerns exporting data to the accompanying program NorRT60 (via Clipboard), and the following two items concerns a separate window allowing the user to make a report document in a standard Rich Text Format (.rtf).

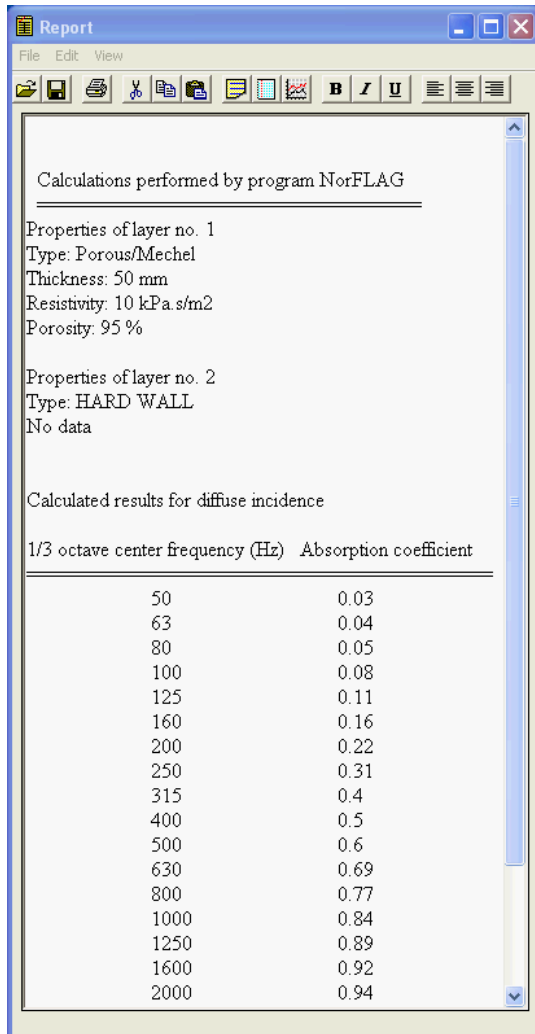
Menu		Shortcut	Description
Save configuration (Example in Annex A)		None	Saves the configuration and all parameters for the layers to a file. The file name is given by the user with the extension ".lag"
Open configuration (Example in Annex A)		None	Opens a file with a formerly saved configuration. Calculations according to the given configuration are performed and results displayed.
Save layer data		None	Saves the user name and all parameters for a single layer to a file. The file name is given by the user with the extension ".alg"
Export results	Plain text	Ctrl T	The current calculated results, together with data for the configuration, are exported to a text file (ASCII) with the extension ".txt". Data that are not relevant in a given configuration, e.g. the sound transmission index when a HARD WALL is included, are set equal to an arbitrary high (negative) number.
	MS Excel	Ctrl E	The current calculated results, together with data for the configuration, are exported to a Microsoft Excel-file with the extension ".xlsx". The option only works if the program Excel™ is installed on the computer.
Export data to NorRT60		None	Copies calculated absorption coefficients in one-third-octave bands to the Clipboard. Intended for exporting data to program NorRT60, calculating reverberation time.
Make report		None	Hides the calculation window and opens up a report window with a text box (.rtf – format) in which the user may import configuration data, results tables and the graphical picture. A description is given below, see Section 5.1.1
Report window		None	Shows the current report window. Hides the calculation window.
EXIT		None	Terminates the program on confirmation.

NOTE 1 A proper saving of the configuration assumes that a calculation has been performed, i.e. the configuration saved is the last one calculated.

NOTE 2 When exporting results calculated in one-third-octave bands one will be offered a choice to add octave-band data to the file.

5.1.1 Making a report

The menu **Make report** opens up a new window, see *Figure 5-1* below, allowing the user to make a report specifying the actual configuration including all parameters for the layers, a copy of the graphical picture and also a table of the results. The latter is limited to one-third-octave band results. If need be, the results for all frequency lines may also be included, a procedure which is outlined below.



The report, see *Figure 5-1*, has three menus, **File**, **Edit** and **View** and a toolbar. Most of the submenus are reflected in this toolbar. The **File** menu has the following items

- Open...
- Save as...
- Print
- Calculation window
- Close

The first two submenus will open up a Microsoft window for opening/saving files. The first option is included if need be to use a formerly saved report file (or a text file) as the basis for a new report. The save option saves the report as an rtf-file.

The print option opens up a standard print window allowing the user to directly print the report on an attached printer. The user can process the report file in a text-processing program. As a consequence, the toolbar offer only a limited number of

Figure 5-1 The report window where the layer properties and one-third-octave results are imported

processing options; i.e. font type and aligning in addition to the standard cut, copy and paste. The latter items are also found under the **Edit** menu.

Furthermore, the submenu Calculation window will hide the report window and revert to the main calculation window for further calculations, the results of which may be added to the report. The Close option will, after confirmation, close the report window (without saving).

The **Edit** menu has in addition to the common options of editing (undo, cut, copy and paste) three special paste commands:

- Paste layer properties
- Paste diagram
- Paste one-third-octave band results

These commands paste a list of the layer properties, the diagram and the results of a one-third-octave band calculation; the latter only if this option is chosen in the main calculation window. These commands are also called using the toolbar buttons to the right of the paste button. In the upper part of *Figure 5-1* an example of a property list is shown, in the lower part the result of a one-third-octave band calculation.

If need be to paste any of the results calculated for single frequency lines the procedure will be a little more involved. The first step is to export the results either to a text file or directly to a Microsoft Excel file. These options are found in the submenus under **Export results** in the **File** menu in the main calculation window. The text file data may easily be imported into a spread sheet, e.g. Microsoft Excel or similar, edited and pasted into the report using the general copy and paste procedure. Finally, the **View** menu controls the toolbar and the status line.

5.2 THE ADD LAYER MENU

The submenus offer the choice of adding the following type of layer:

- Air
- Porous facing
- Porous layer
 - Allard-Johnson (may be modified to a “limp” model)
 - Attenborough
 - Delany/Bazley
 - Komatsu
 - Mechel
 - Sgard (Doubly porous)
 - Wilson
- Slotted plate
 - Regular long slots
 - Rectangular slots
 - Conical long slots
- Perforated plate
 - Regular holes
 - Regular holes w/fabric
 - Conical holes
 - Microperforated
- Limp mass
- Solid plate (panel)
 - Thin plate
 - Thick plate (elastic)
 - Corrugated plate
 - Cladding
 - Wave
 - Sandwich
- Structural bridges
 - Stiff
 - Flexible
- HARD WALL (Rigid backing)
- Add layer from file

Except for the last item, clicking on one of these submenus brings a layer of the specified type into the configuration list box. Using the last item, a formerly saved layer is placed in the list box. **The layer is added below a marked layer. If no layer is marked it will be added at the end of the list.** A short description of each of these layers is given in the table below together with a reference to a Section under which to find a more detailed explanation of the various models used.

Submenu		Short cut	Description
Air		None	This layer has its thickness as the main parameter with a default value of 50 mm. There is also the possibility to specify an attenuation coefficient. See details under the Section 5.2.1
Porous facing		None	A layer simulating a thin porous layer or fabric normally attached to a thicker porous material, e.g. mineral wool. See details under Section 5.2.2.
Porous layer	Allard-Johnson	None	A rigid frame model with a total of six parameters. The shape of the pores and their interconnections are characterised by parameters called viscous length and thermal length. May be modified into a limp frame model. Details are given under the Section 5.2.3.1
	Attenborough	None	Theoretical model after Attenborough using a total of five parameters. Two of these parameters, a factor s_f describing the form of the pores and the flow resistivity r , are input as one parameter $s_f^2 \cdot r$. Details are given under the Section 5.2.3.2.
	Delany/Bazley	None	Porous material described by the empirical model after Delany and Bazley. The model has two parameters, the thickness and the flow resistivity and presupposes porosity near to 100%. On details, see under the Section 5.2.3.3
	Komatsu	None	Porous material described by a model by Komatsu. Similar to the Delany/Bazley model the flow resistivity is the only material parameter and presupposes porosity near to 100 %. On details, see under Section 5.2.3.4.
	Mechel	None	Porous material described by a model after Mechel. Compared to the model after Delany and Bazley it has the porosity as an additional parameter (see Note 1 below table). The model is a combination of a theoretical model for the behaviour at low frequencies and an empirical model for the higher frequencies. See details under the Section 5.2.3.5

	Sgard et al. (Doubly porous)	None	Model for a porous material perforated by holes of circular shape given by Sgard et.al. Presupposes relatively large holes, diameter $> 20 - 30$ mm. Setting the diameter equal zero, the model changes to the one by Allard-Johnson, see details in Section 5.2.3.6.
	Wilson	None	Theoretical model viewing thermal and viscous diffusion in porous media as relaxational processes. The relaxational parameters used in the program are the ones mimicking the model of Delany/Bazley. Details are given in Section 5.2.3.7.
Slotted plate	Regular long slots	None	Conventional slotted plate constructed from beams of rectangular cross section and having sharp edges, e.g. a wooden slatted panel. See details under the Section 5.2.4.1
	Rectangular slots	None	Plate with a regular pattern of rectangular shaped slots, see details under Section 5.2.4.2
	Conical long slots	None	Slotted plate, as the regular long slots type above, but constructed from beams of trapezoidal cross section. See details under Section 5.2.4.3
Perforated plate	Regular holes	None	Plate or panel perforated with holes of circular shape; typically metal panels, plasterboard or chipboard panels. See details under the Section 5.2.5.1.
	Regular holes w/ fabric	None	A combination of a plate or panel as described above and a fabric described as a porous facing; see the second row in this table. Further details are found in Section 5.2.5.2.
	Conical holes	None	Panel perforated with holes of conical shape; typically relatively thick panels ($> 9 - 10$ mm), e.g. plasterboard, chipboard etc. See details under the Section 5.2.4.3
	Micro-perforated	None	Plate, panel or foil perforated with holes of circular shape but the diameter of the holes is less than 0.5 mm. Details are given under the Section 5.2.5.4
Limp mass		None	A mass layer characterised by its thickness and density only. Represents typically a thin layer of plastics or metal. See details under the Section 5.2.6.
Solid plate (panel)	Thin plate	None	A thin plate or panel characterised by its bending stiffness, mass and loss factor. See details under the Section 5.2.7.1
	Thick plate (elastic)	None	A solid elastic plate characterised by the same material properties as the thin plate but allow for thickness deformation. See details under the Section 5.2.7.2

	Corrugated plate	Cladding	None	A corrugated sheet cladding of the type illustrated in <i>Figure 5-20 a)</i> in section 5.2.7.3.
		Wave	None	A corrugated sheet having corrugations of a sinusoidal wave type. See <i>Figure 5-20 b)</i> and details under section 5.2.7.3.
	Sandwich		None	Sandwich panel construction with three layers, i.e. two identical thin face sheets with a thicker core. All layers are isotropic and homogeneous. See details under the Section 5.2.7.4
Structural bridges	Stiff		None	Introduces stiff structural connections, studs or “ties”, between two outer plate layers in a double plate construction. Restricted to two types of thin plate or corrugated plate constructions. See details under Section 5.2.8 and 5.2.8.1
	Flexible		None	Simulates flexible types of structural connections between plates in double wall constructions. See details under Section 5.2.8 and 5.2.8.2.
HARD WALL (Rigid backing)			None	An infinitely stiff wall. It is typically used to represent a termination for an absorbent placed against the ceiling or wall in a room. This layer has no parameters.
Add layer from file			Ctrl L	A formerly saved layer with user specified name and parameter data is input from a file (with extension .alg) and placed in the configuration list box.

NOTE 1. Porous/Mechel layer: Actually, the model for this layer also applies to high porosity materials only, even if the porosity is a parameter. Mechel, see reference under Section 5.2.3.5, recommends setting this parameter to 95%, which he assumes applies to most commercial fibre materials.

NOTE 2. Thick plate and Sandwich layer: Please observe that these “layers” may only be directly coupled to the fluid layers, i.e. either the air layer or the porous ones. However, a number of thick plates may be coupled; please see Section 5.2.7.2.

NOTE 3. Inclusion of structural bridges will only affect the transmission results. Any possible effects on the absorption or impedance are not accounted for.

5.2.1 The air layer

The layer is specified by its thickness in mm and characterised by the specific impedance (characteristic impedance) $\rho_0 c_0$ of air, where ρ_0 is the density and c_0 is the speed of sound. These quantities are given the values applicable for a temperature of 20 °C, i.e. ρ_0 and c_0 take on the values 1.21 kg/m³ and 343 m/s. The characteristic impedance is then approximately 415 Pa·s/m.

There is also an option to introduce attenuation in the layer by a power attenuation coefficient m (km⁻¹), i.e. the wave intensity is reduced by the factor $\exp(-mx)$, where x the

distance in km. The corresponding intensity level is reduced by approximately $4.343 \cdot m$ (dB/km). Please observe that this input parameter is a constant value (frequency independent). General data for the coefficient $\alpha = 4.343 \cdot m$ (dB/km) as a function of frequency, air temperature and humidity is tabled in ISO standard 9613–1.

5.2.2 Porous facing

Several types of porous material described by the models below have in practice an outer facing of some kind of fabric, e.g. glass fibre, to prevent contamination of loose fibres from the porous material. The facing gives a small increase in the thickness of the absorbent but may lead to an overall improvement in the absorption. A model given by Rebillard *et.al.*; see reference below, is used. It should be observed that in the implementation we assume that the facing has negligible stiffness and furthermore, is “unbounded” when attached to a porous

layer. The window specifying the material properties of the facing is shown in *Figure 5-2*. For a thin layer, the tortuosity parameter has only a minor effect and may normally be left at the default value 1.0.

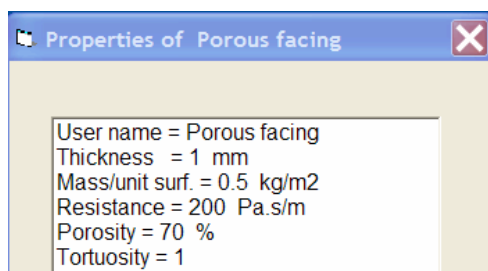


Figure 5-2 The property window for a porous facing

Reference:

P. Rebillard *et.al.* (1992) The effect of a porous facing on the impedance and the absorption coefficient of a layer of porous material. *J. Sound and Vibration*, **156**, 541–555.

5.2.3 Porous layers

The program offers a choice of using six different models for describing a homogeneous porous layer. These models use one or more material parameters to calculate the acoustical properties. In addition, there is a model for a so-called double porosity material, here implying that the material is perforated with relatively large holes. However, as also pointed out in the introduction, the material is in all models treated as an equivalent fluid, i.e. the elastic properties are not taken into account and the models may not properly describe foam materials.

5.2.3.1 Model by Allard and Johnson with a “limp” model modification.

The basic rigid frame model is thoroughly explained in the book by Allard from 1993; see the reference [1] below, where the model is summarised on page 92. One should note that in the literature one often finds this model denoted the JCA (Johnson-Champoux-Allard) model. Furthermore, one should consult the second edition, the book by Allard and Atalla; see the reference [2] below, for the range of porous models existing, described as elastic, rigid or limp. The basic Allard/Johnson model used here introduces two parameters to characterise the shape of the pores in the material. These parameters are termed characteristic *viscous length* Λ and characteristic *thermal length* Λ' . The advantage of this description is that, using high frequency sound (some hundred kHz), one may by measurements determine each of these parameters separately. As an indication of the magnitude of Λ and Λ' will, for foam materials, be in the range of some tenths of μm to some hundred μm .

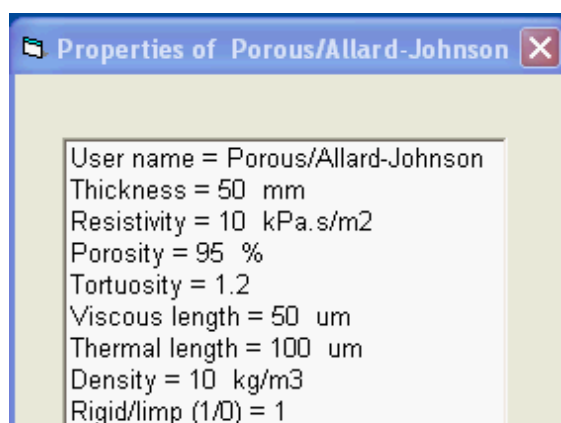


Figure 5-3 The property window for a rigid porous layer using the Allard-Johnson model, where also the limp alternative may be chosen.

The relationship between these two parameters also gives an indication of the pore shape. For a material with pores resembling straight tubes the two parameters will be of the same magnitude. In contrast, if the pores are interconnected by narrow tubes giving high resistance for flow, we will have $\Lambda \ll \Lambda'$.

Later work has shown that some precautions have to be taken when using the equivalent fluid model, taking the frame as being motionless. A rigid body motion may be observed in transmission phenomena, which may be accounted for by using a so-called limp frame equivalent fluid model; see e.g. reference [4] below. This modifies the effective density of the porous material taking into account its total apparent mass. The question is how to decide whether a limp model or a rigid one is appropriate. A criterion is offered by Doutres et.al. ; see reference [5] below, by a critical value of a parameter denoted FSI (Frame Stiffness Influence). In effect, one then needs to calculate the bulk modulus of the frame.

The window for specification of the parameters for this model is shown in *Figure 5-3*. Setting the last parameter to zero, the rigid model is converted to a limp one, which means that the density parameter is important.

Lastly one should observe, as stated in the introduction, that in most cases plastic foam materials need additional parameters for a complete description of the acoustical behaviour. The program will only give correct results when the elastic properties of the frame material may be neglected. As a rule of thumb, for foams layers 25 - 100 mm thickness, the elastic properties may strongly influence the acoustic data below 500 - 1000 Hz.

References:

- [1] J.F. Allard (1993) *Propagation of sound in porous media*. Modelling sound absorbing materials. Elsevier Applied Science, London and New York.
- [2] J.F. Allard and N. Atalla (2009) 2nd Ed. *Propagation of sound in porous media*. Modelling sound absorbing materials. John Wiley & Sons.
- [3] Ph. Leclaire, L. Kelders, W. Lauriks, M. Melon, N. Brown, B. Castanede (1996) Determination of the viscous and thermal characteristic length of plastic foams by ultrasonic measurements in helium and air. *J. Appl. Physics* **80**, 2009 - 2012.
- [4] R. Panneton (2007) Comments on the limp frame equivalent fluid model for porous media. *J. Acoust. Soc. Am.* **122**, EL217.
- [5] O. Doutres, N. Dauchez, J.-M. G  nevaux and O. Dazel (2009). A frequency independent criterion for describing sound absorbing materials by a limp frame model. *Acta Acustica united with Acustica*, **95**, 178 – 181.

5.2.3.2 Model by Attenborough

The work of Attenborough is primarily directed towards modelling ground impedance for the purpose of predicting outdoor sound propagation. He introduces a parameter s_f , the pore shape factor, to account for the shape of the pores in the material. One is not, however, able to measure this parameter separately and it must then be estimated by other means. In the program it is input in combination with the flow resistivity as a product $s_f^2 \cdot r$. An additional parameter to describe the pore orientation in the material, the *sinuosity* or more commonly termed the *tortuosity*, is also introduced. The window specifying the material parameters for this model may be seen from Figure 5-4. More details concerning this model may be found in the reference below. Please observe that Attenborough uses the symbol q^2 for tortuosity.

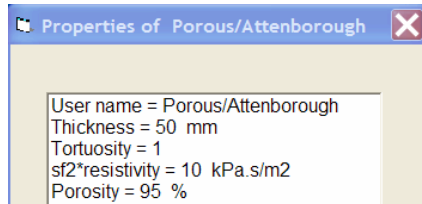


Figure 5-4 The property window for a porous layer using the Attenborough model

Reference:

Attenborough, K. (1985) Acoustical impedance models for outdoor ground surfaces, *J. Sound Vib.* **99**(4), 521 - 544.

5.2.3.3 Model by Delany and Bazley

The model presented by Delany and Bazley, see reference below, is an empirical one based on a large number of measurements on materials having a porosity approximately equal to one (or 100% as used in this program). Using the frequency and the flow resistivity of the material as the only variables they arrived at empirical equations for the complex propagation coefficient Γ and the complex characteristic impedance Z_k of the material which may be written:

$$Z_k = \rho_0 c_0 \left[1 + 0.0571 \cdot E^{-0.754} - j \cdot 0.087 \cdot E^{-0.732} \right]$$

$$\text{and } \Gamma = j \frac{\omega}{c_0} \left[1 + 0.0978 \cdot E^{-0.700} - j \cdot 0.189 \cdot E^{-0.595} \right] \quad \text{where } E = \frac{\rho_0 f}{r}.$$

The quantity r is the flow resistivity in $\text{Pa}\cdot\text{s}/\text{m}^2$; f is the frequency in Hz and ω is the angular frequency in radians/s. Delany and Bazley suggest that the validity of their model is limited to the range $(0.01 < E < 1.0)$. The window specifying the material parameters for a layer using this model may be seen from the Figure 5-5.

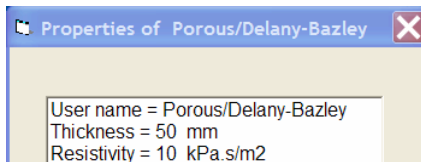


Figure 5-5. The property window for a porous layer using the Delany-Bazley model

Reference: M.E. Delany and E.N. Bazley (1970) Acoustical properties of fibrous materials. *Applied Acoustics* **3**, 105.

5.2.3.4 Model by Komatsu

A more recent simple model, applying to porous materials such as mineral wool, is given by Komatsu. It is claimed to be an improvement of the model of Delany and Bazley and also a later adjustment of this model by Miki; see references below, an improvement both for high and low density materials. Based on measurements on 15 types of glass wool and 9 types of Rockwool, Komatsu presents the following expressions for the characteristic impedance and propagation coefficient

$$Z_k = \rho_0 c_0 \left[1 + 0.00027 \cdot (2 - \lg E_k)^{6.2} - j \cdot 0.0047 \cdot (2 - \lg E_k)^{4.1} \right]$$

and $\Gamma = \frac{\omega}{c_0} \left[0.0069 \cdot (2 - \lg E_k)^{4.1} + j \cdot (1 + 0.0004 \cdot (2 - \lg E_k)^{6.2}) \right]$ where $E_k = \frac{f}{r}$.

The property window is equal to the one for the model of Delaney and Bazley.

References:

1. T. Komatsu (2007) Improvement of the Delany-Bazley and Miki models for fibrous sound-absorbing materials. *Acoust. Sci. & Tech.* **29**, 121-129.
2. Y.Miki (1990) Acoustical properties of porous materials – modifications of Delany-Bazley models. *J. Acoust. Soc. Jpn.* **11**, 19-24.

5.2.3.5 Model by Mechel

Mechel presents an extension of the Delany-Bazley model where he gives different equations depending on frequency. The model uses a theoretical expression for the behaviour at low frequencies combined with a curve fitting procedure to experimental data to predict the behaviour in the middle and the high frequency ranges. The model has the porosity as an additional parameter as compared with the Delany-Bazley model. Actually, the model for this layer also applies to high porosity materials only, even if the porosity is a parameter. The porosity parameter will only affect the low frequency part. Mechel, see the second reference below, recommends setting this parameter to 95%, which he assumes applies to most commercial fibre materials.

We omit the presentation of the equations here, which can be found from the references below. The window specifying the material parameters for a layer using this model may be seen from *Figure 5-6*.

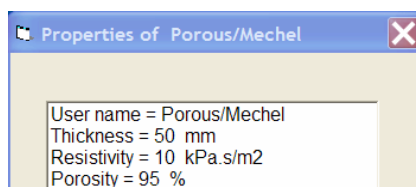


Figure 5-6. The property window for a porous layer using the Mechel model

References:

1. F.P. Mechel (1976) Ausweitung der Absorberformel von Delany und Bazley zu tiefen Frequenzen. *Acustica* **35**, 210 - 213.
2. F.P. Mechel (1988) Design charts for sound absorber layers. *J. Acoust. Soc. Am.* **83**, 1002 - 1013.

5.2.3.6 Model by Sgard et.al. Double porosity materials

Of great interest in the later years have been porous materials with meso-perforations, also called “double porosity materials”, as they are made up of two interconnected networks of pores of quite different size. In practice, such materials contains perforations, normally holes, with a characteristic size much larger than the pores in the material; i.e. a lateral dimension of centimetres. Due to a diffusion effect in the meso-pores, enhancement of the acoustic properties may be achieved in given frequency ranges, although there will be reduced effect in other frequency ranges as compared with the non-perforated material. An example is shown in *Figure 5-8* using the default data given in the property window shown in *Figure 5-7*, terminating the material with a hard backing. A further example is given in Annex I, where predicted results are compared with measurement data.

The model implemented in the program is the analytical model given by Sgard et.al; see reference below. It should be noted that there are restrictions when it comes to combinations with other layers. The effect of other types of layers, except for the air layer, directly in front of the double porosity layer is not clear. Furthermore, the following layer must either be the air layer or a hard backing. As the other porous models, used in this program, structural effects of the material are not accounted for; the material has a stiff skeleton. It should be mentioned that later developments also include structural effects; see e.g. the reference in Annex I. Furthermore, the inclusions may not only be air-filled but contain a different porous material etc.

It should be noted that compared to the model of Allard and Johnson; see Section 5.2.3.1 above, there is another thermal parameter included in the properties list, the static thermal permeability with dimension m^2 . To roughly compare results with the non-perforated material, setting the diameter of the holes to zero, the model reverts to the rigid one by Allard and Johnson, as shown by the dotted curve in the example *Figure 5-8*.

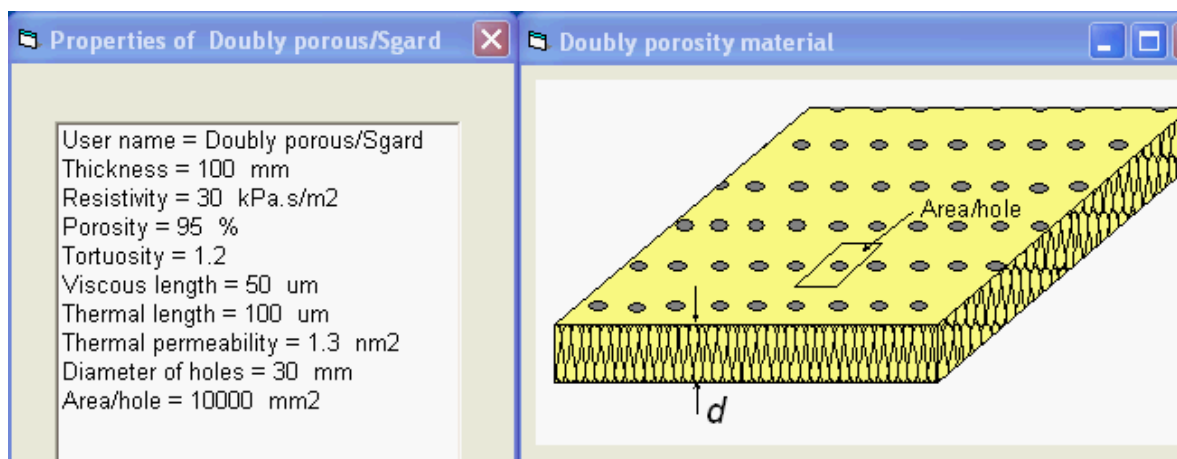


Figure 5-7 Properties window for a double porosity material.

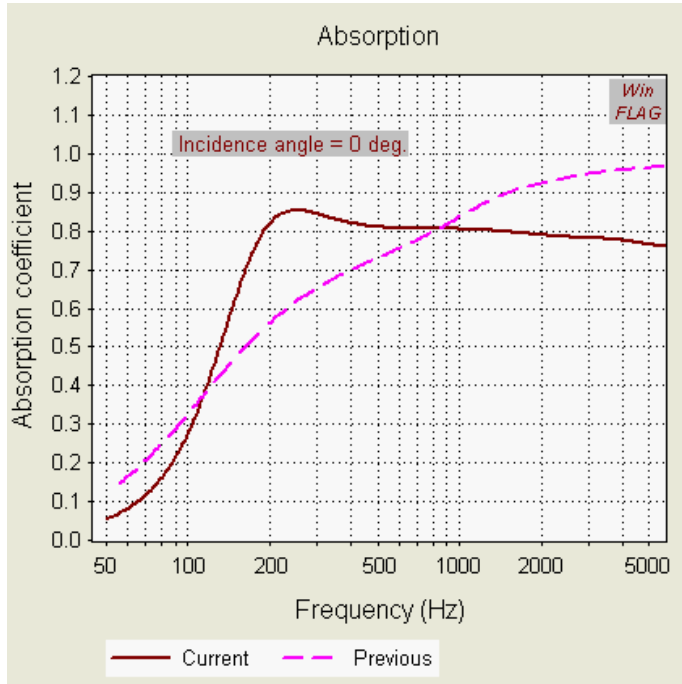


Figure 5-8 Absorption coefficient for a double porosity material with a hard backing using default data. Dotted curve shows result of non-perforated material.

References:

F.C. Sgard, X. Olny, N. Atalla and F. Castel (2005). On the use of perforations to improve the sound absorption of porous materials. *Applied Acoustics* **66**, 625 - 651.

5.2.3.7 Model by Wilson

Unlike the models for porous materials presented above, the model by Wilson is based on viewing the viscous and thermal diffusion in porous media as relaxational processes. The parameters determining these processes and thereby the acoustic behaviour are the characteristic times τ_{vor} and τ_{ent} , where the indices “vor” and “ent” signifies vorticity (viscous diffusion) and entropy (thermal diffusion). The general equations for the complex propagation coefficient Γ and the complex characteristic impedance Z_k of the material are; see reference below

$$Z_k = \rho_0 c_0 \frac{q}{\Omega} \left[\left(1 + \frac{\gamma - 1}{\sqrt{1 + j\omega\tau_{\text{ent}}}} \right) \left(1 - \frac{1}{\sqrt{1 + j\omega\tau_{\text{vor}}}} \right) \right]^{-\frac{1}{2}},$$

$$\Gamma = \frac{\omega}{c_0} q \left[\left(1 + \frac{\gamma - 1}{\sqrt{1 + j\omega\tau_{\text{ent}}}} \right) / \left(1 - \frac{1}{\sqrt{1 + j\omega\tau_{\text{vor}}}} \right) \right]^{+\frac{1}{2}}$$

where q and Ω are the tortuosity and the porosity, respectively. Wilson chooses the characteristic times to compare with altogether three other models, among them the Delaney/Bazley model, giving a good fit in the valid frequency range for this model by choosing

$$\tau_{\text{vor}} \cong 2.1 \frac{\rho_0}{\sigma} \quad \text{and} \quad \tau_{\text{ent}} \cong 3.1 \frac{\rho_0}{\sigma},$$

setting both the tortuosity and porosity equal to one (1.0). This is the model implemented in the present program and the property window is equal to the one used for the Delany/Bazley model.

Reference:

D.K. Wilson (1997) Simple, relaxational models for the acoustic properties of porous media. *Applied Acoustics* **50**, 171 - 188.

5.2.4 Slotted plate (Slatted panel)

These types of layers are intended to be included in a resonance absorber composed of a slotted plate placed at a distance from a ceiling or a wall, i.e. a common absorber system is the plate, airspace with or without a porous layer and a hard backing wall. In the normal case the slotted plate could typically be an assemblage of parallel sharp edged beams (slats) of rectangular cross section with a specified thickness and width. This is commonly called a slatted panel. However, a calculation procedure should also apply to thin perforated panels, e.g. metal panels so the common name “slotted plate” is used in the menu. These cases are chosen using the submenu’s “Regular long slots” or “Regular rectangular slots”, where the latter implies that the slots may be quite short, in fact equivalent to a perforated plate with holes, see section 5.2.5. Using the last submenu “Conical long slots”, the cross section of the beams (slats) will be trapezoidal.

5.2.4.1 Regular long slots

The distance between the beams is characterised by the *slot width*, see the window for the specification of parameters shown in *Figure 5-9* and the width of the beams goes into the parameter *centre-to-centre distance* between slots. The density of the material is also part of the specification going into the calculation of the equivalent mass impedance of the plate. Normally, the influence of the latter impedance will be very small.

To obtain a high absorption coefficient for a resonance absorber the panel must be combined with a porous layer or a fabric placed close to the slots, this to give the necessary resistance component. (An exception to this rule is by using the so-called microperforated plate or panel, see below). If a fabric is used, the total resistance (in Pa·s/m) must be specified.

In case one is using a porous layer in the air space directly behind or in front of the slotted plate there is also the possibility to add an extra *resistance correction* to the data. This is a parameter that should take on values between zero and one. This indicates that one is adding a resistance component equal to the total resistance of the porous layer having a maximum thickness of one *end correction* for the slots. The rationale behind this option is that the acoustical properties of the panel are not independent of a close-coupled porous layer. Further explanation is given in the next section. The default value of this parameter is zero and it should only be changed if warranted by user experience.

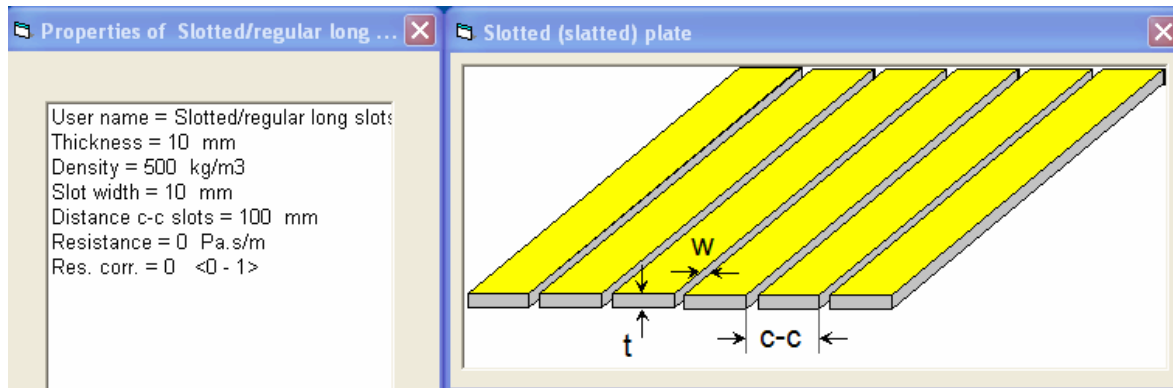


Figure 5-9. The property window for a regular slotted plate

Important notice! For wide slots combined with a very high percentage open area, say above 30–40 %, this model may give unreliable results for frequencies above the fundamental resonance frequency. Information on the percentage open area will be given when updating the relevant parameters.

Reference:

U.R. Kristiansen and T.E. Vigran (1994), On the design of resonant absorbers using a slotted plate. *Appl. Acoustics* **43**, 39 - 48.

(Please observe that there is a misprint in equation (6) in the article. The matrix element a_{12} should be $W \cdot \sinh(D)$)

5.2.4.2 Regular rectangular slots

This case applies to panels or perforated plates having slots in a regular pattern, as shown in the sketch to the right in *Figure 5-10*. In addition to the slot width w and centre-to-centre distance between slots for the case in the preceding section, the slot lengths (L) and the centre-to-centre distance in two directions are now additional parameters. This is seen from the window for specifications of the parameters in the left part of the figure.

The model used here is based on the exact expression for the so-called complex density and compressibility of air in a tube of rectangular shape, see reference [1] below. For the so-called end correction of such a slot, a low frequency approximation of the radiation impedance, corrected for the mutual influence of the neighboring slots is used [2, 3]. As for this model, there should be no restrictions as for the dimensions of the slit width w or for the length L .

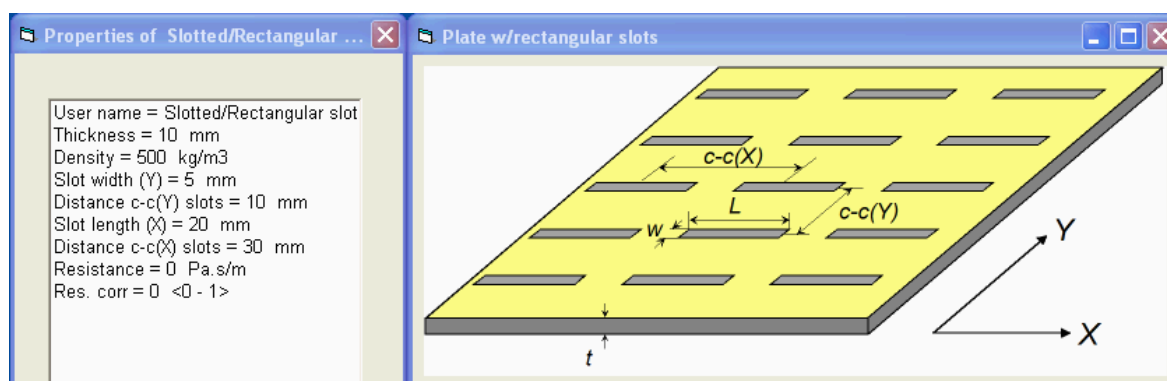


Figure 5-10 The property window and a sketch of a perforated plate with rectangular slots.

References:

- [1] M. R. Stinson, The propagation of plane sound waves in narrow and wide circular tubes, and generalization to uniform tubes of arbitrary cross-sectional shapes. J. Acoust. Soc. Am. 1991; **89**: 550–558.
- [2] U. Ingard, On the theory and design of acoustic resonators. J. Acoust. Soc. Am. 1953; **25**: 1037–1061.
- [3] T.E. Vigran, The acoustic properties of panels with rectangular apertures. J. Acoust. Soc. Am. 2014; **135**: 2777–2784.

5.2.4.3 Conical (wedge-shaped) long slots

Instead of using a panel which is an assemblage of beams (slats) of rectangular cross section, see Section 5.2.4.1 above, one may use beams having a trapezoidal cross section, i.e. the slots will have a conical shape, see Figure 5-11. As shown in the reference below this will, for relatively thick panels, give resonance absorbers acting over a broader frequency range as compared with the regular ones. Due to the shape of the slots the window for specifying the parameters, see Figure 5-12, will contain data for *slot width* on the entrance side as well as on the exit side. The same apply to an added resistance layer. This could be placed on either side of the panel.

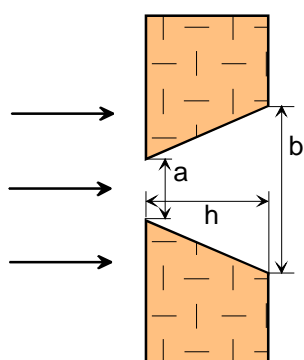


Figure 5-11 Conically shaped slot in a panel of thickness h . The width on the entrance and exit side is a and b , respectively.

The conical angle one may use is restricted upwards to approximately 30 degrees. The slot width on the exit may not be equal (or smaller) than the entrance width but calculations may be performed with only a fractional difference, i.e. in the order of 1/10 % so one may well apply this model to regular slotted panels.

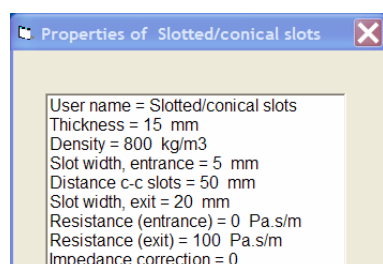


Figure 5-12 The property window for the slotted plate with conical slots.

The model used is also more advanced than the one used for regular panels in Section 5.2.4.1, where the air in the slot is treated as a concentrated mass of air. This implies that now the real wave movement in the slots is calculated which may show effects at higher frequencies due to thickness resonances.

A correction for the effect of a porous layer behind the panel is included using the parameter *Impedance correction*. This will take effect setting this parameter different from zero. The reason for this name is that the routine calculates the so-called radiation impedance of the slot looking into the porous layer instead of treating this layer as plain air. Experience shows, see e.g. the paper by Kirby and Cummings in the reference below that using such corrections easily overestimates the effect of the porous layer. The correction used here is therefore empirically set to use the mean value of the impedance in the two cases, air and porous medium.

References:

1. Vigran, T. E. (2004) Conical apertures in panels; Sound transmission and enhanced absorption in resonator systems. *Acta Acustica united with Acustica*, **90**, 1170 – 1177.
2. Kirby, R and Cummings, A. (1998) The impedance of perforated plates subjected to grazing flow and backed by porous media. *Journal of Sound and Vibration*, **217**, 619 – 636.

5.2.5 Perforated plate

As for the slotted plate, the perforated plate is intended for use in a resonance absorber. The program offers the choice of three types of plates: regular cylindrical holes, holes of conical shape and micro perforation. The latter means that the diameter of the holes is less than 0.5 mm.

5.2.5.1 Regular holes

The plate in this case is typically a thin metal plate perforated by holes. The program assumes that the shape of the holes is cylindrical. The model may also be used for thicker plates of other materials, e.g. plasterboard, chipboard or similar. The window for specifying the parameters has already been presented; see *Figure 4-2*, but is also shown below. Obviously, the parameters resemble the ones for the slotted plates. Please observe that the notice in Section 5.2.4.1 above, concerning the percentage open area, also applies to this model of a perforated plate.

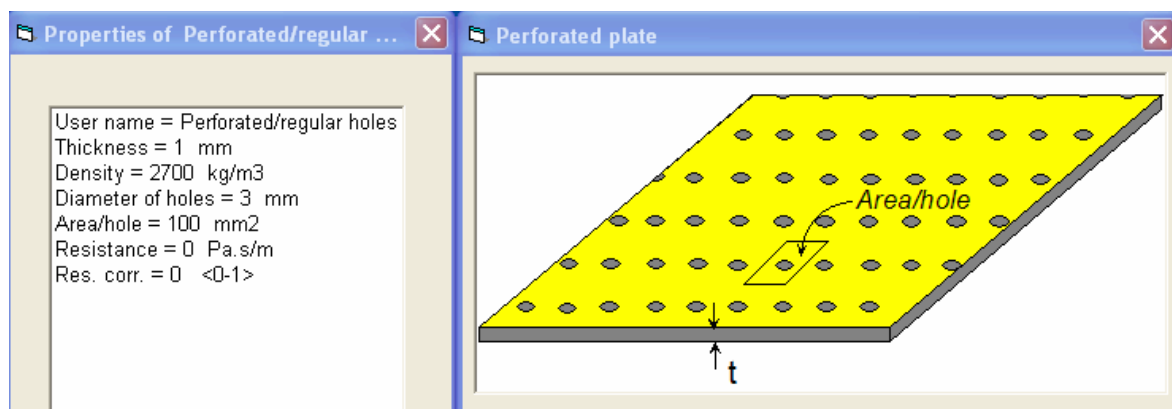


Figure 5-13 Sketch and property window for a plate perforated with cylindrical holes in a regular pattern.

5.2.5.2 Regular holes with fabric

A slightly improved model of a perforated plate, when combined with a resistance fabric on the back side, is constructed by defining a layer being a combination of a perforated plate and a layer of the type “porous facing” as outlined in Section 5.2.2. Measurement results from a standing tube have revealed that the predictions using such a layer, combined with an air cavity, fits slightly better than the model above when it comes to the frequency of maximum absorption, i.e. when applying the same resistance value. The property window for this layer is given in *Figure 5-14*.

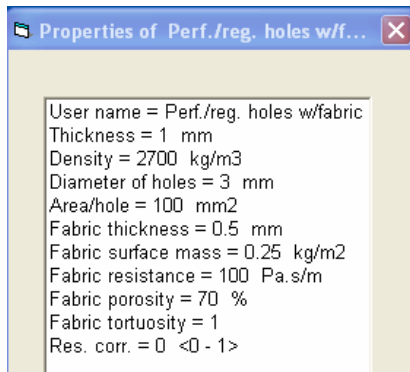


Figure 5-14. Property window for the combination of a perforated plate with holes and a porous layer, the latter as described in Section 5.2.2.

5.2.5.3 Conical holes

Analogous to the slotted plate with conical slots this layer represents plates perforated with conical holes, i.e. the holes have a shape which may be illustrated by *Figure 5-11* but now the dimensions a and b are the diameter of the hole at the entrance and exit side, respectively. The window for specifying the parameters, see *Figure 5-15*, is therefore quite similar to the one for a slotted panel with conical slots.

Again, the conical angle one may use is restricted upwards to approximately 30 degrees but calculations may be performed with only a fractional difference between the diameters of the holes on the entrance and exit side.

The parameter *Impedance correction* works in the same way as for conical slots; the radiation impedance seen from hole into a porous layer is modified. Annex D gives an example on measurements and calculations on resonator panels comparing panels using conically shaped holes and regular cylindrical ones.

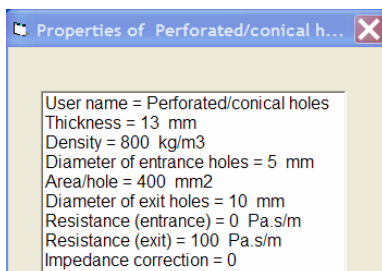


Figure 5-15 The property window for the perforated plate with conically shaped holes.

5.2.5.4 Microperforated

This plate is in principle equal to an ordinary perforated plate described above in Section 5.2.5.1 but with an important exception: the diameter of the holes should typically be less than 0.5 mm. A porous layer or a fabric is then superfluous to get a necessary resistance component for such a plate used in a resonance absorber. As shown in *Figure 5-16*, the window for specifying the parameters has never the less the option for adding a fabric with a given flow resistance. The density of the material is also part of the specification going into

the calculation of the equivalent mass impedance of the plate. Normally, the influence of the latter impedance will be very small using metal plates. However, due to the advent of micro-perforated plastic sheets acting as membranes this may be an important parameter. For an example, see Annex C.

An analytical expression to calculate the impedance of the holes in such a plate has been known for nearly hundred years but the idea to exploit the principle to make a practical acoustical absorber was put forward by Maa in 1987. The reference given below is a later article by the same author that also has a number of references to other papers on the subject.

It should be pointed out that the present program does not use the approximate formulas for the impedance given by Maa but the calculations are based on the full analytical solution which includes Bessel functions with complex argument. This does not imply, however, that the accuracy is very much better than when using the approximate formulas.

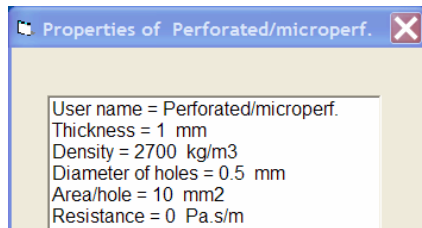


Figure 5-16. The property window for a microperforated plate.

Reference:

Maa, D. Y. (1998) Potential of microperforated panel absorber. *J. Acoust. Soc. Am*, **104**(5), 2861 - 2866.

5.2.6 Limp mass

The layer is primarily intended to represent a thin, impermeable sheet (plastic, metal etc.) or a very thin plate or panel where the bending stiffness is negligible. It may then be used to calculate the absorption of membrane absorbers, i.e. when this layer is combined with an air space in front of a hard backing wall. However, the normal use will be to calculate the effect of covering a porous material with an impermeable thin layer. In the specification of the input parameters, see *Figure 5-17*, there is also the opportunity to specify a resistance component added to the mass. The size of this component must wholly depend on user experience.

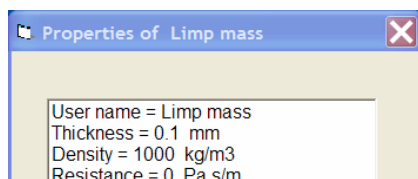


Figure 5-17. The property window for a mass layer (limp mass)

5.2.7 Solid plate (panel)

The program offers calculations with five different types of panel. The first two models a single solid plate using so-called thin plate and thick plate theory, respectively. The first normally implies that the wavelength of bending waves is larger than approximately six times the thickness of the plate, whereas the second allow for thickness deformation of the plate. This may result in dilatational resonances reducing the sound reduction index of the panel.

The third submenu choice is corrugated plates, of which two types are implemented; either a simple wave-corrugated one or the one normally called cladding with trapezoidal corrugations. The last submenu choice is a sandwich panel. In relation to this program the sandwich panel is a special case. The layer is actually a combination of three separate layers, a core with two face sheets; see sketch in *Figure 5-22*.

5.2.7.1 Thin plate

As stated above, the model used for this layer is based on thin plate theory, which normally implies that the wavelength of bending waves in the plate is larger than approximately six times the thickness of the plate. The so-called wall impedance Z_w of a plate, i.e. the difference in sound pressure across the plate divided by the velocity of the plate, may then be written

$$Z_w = j\omega m \left[1 - \left(\frac{f}{f_g} \right)^2 \cdot (1 + j\eta) \sin^4 \varphi \right],$$

where m , η and f_g are the mass pr unit area, the loss factor and the coincidence frequency, respectively. φ is the angle of the incident plane wave and f and ω symbolise the frequency in Hz and the angular frequency in radians pr second. The coincidence frequency is given by

$$f_g = \frac{c_0^2}{2\pi} \sqrt{\frac{m}{B}},$$

where the mass pr unit area m and the bending stiffness B may be calculated from the density of the material ρ and the plate thickness h , respectively from the elastic modulus (Young's modulus) E , Poisson's ratio ν and the thickness using the equations

$$m = \rho \cdot h \quad \text{and} \quad B = \frac{E}{1-\nu^2} \cdot I = \frac{E}{1-\nu^2} \cdot \frac{h^3}{12}.$$

Here the I is symbolising the area moment of inertia per unit width. The window for specification of the necessary input parameters is shown in *Figure 5-18*.

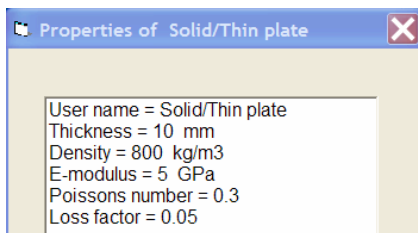


Figure 5-18. The property window for a thin solid plate (panel)

5.2.7.2 Thick plate (elastic)

The property window for the thick plate is, apart from the default values, identical to the property window for the thin plate or panel.

As stated in the introduction we shall need four physical variables, e.g. the particle velocity and the stress in two directions to describe the relationship between the input and output for a thick (homogeneous and isotropic) elastic plate or wall. In another words, we have to use a 4x4 matrix instead of the simple 2x2 matrices generally implemented in NorFLAG.

Explicit analytical expressions for the sound reduction index (transmission loss) of single thick plates (walls) may be found in the reference below, Ljunggren (1991). However,

to include the calculations in the general layout of the program an approach based on the general theory of layered elastic media is used, see the reference Folds and Loggins (1977). The latter article gives expressions for all 16 elements of the matrix that describe the relationship between the input and output particle velocity and stresses in two directions for a single layer. Coupling a number of such elastic layers, the total 4x4 matrix is evaluated and finally reduced to a 2x2 matrix when fluid layers appear on both sides of the total elastic combination. Examples, showing the sound reduction index for three-layer elastic configurations, are shown in the Annexes H1 and H2. In the former, examples of laminated glazing with PVB (polyvinyl butyaryl) are shown, whereas the latter gives an example of a multi-layered panel; a steel plate, a dense mineral wool layer and a laminated plate being glued together.

When calculating the sound reduction index of configurations involving single plates it is advisable to compare results using both models. Normally, the differences should be small for most building materials but one should use the thick plate option if the results diverge significantly in an important frequency range. An example on such comparison was presented under Section 4.2; see *Figure 4-6*.

The old “rule of thumb” on the frequency limit of using thin plate theory is that the bending wavelength in the plate should be larger than six times the plate thickness. As an example, for a 200 mm concrete plate, thin plate theory could be used at frequencies below approximately 1000 Hz. Ljunggren (1991), however, claims that for sound transmission calculations a factor of three (instead of six) may be used. This will, for the 200 mm concrete plate, extend the useful range of thin plate theory to nearly 4000 Hz.

References:

1. Ljunggren, S. (1991) Airborne sound insulation of thick walls. *J. Acoust. Soc. Am.* **89**, 2338 - 2345.
2. Folds, D.L. and Loggins, C. D. (1977) Transmission and reflection of ultrasonic waves in layered media. *J. Acoust. Soc. Am.* **62**, 1102 - 1109.

5.2.7.3 Corrugated plates

Corrugated plates are special cases of orthotropic plates, i.e. plates where the stiffness depends on the direction. As such they differ from all the other “layers” implemented which all are homogeneous and isotropic. This implies that calculating e.g. the sound reduction index for diffuse sound incidence the integration involves two angles, the angle of incidence φ as well as the azimuth angle θ . This is illustrated in *Figure 5-19*.

The advantage of using corrugated panels is their strength compared with a flat panel of the same material and thickness. The drawback is that the insulation properties may be much poorer than for the similar flat panel.

The wall impedance may be written

$$Z_w = j\omega m \left[1 - \left(\frac{f}{f_{g1}} \cos^2 \theta + \frac{f}{f_{g2}} \sin^2 \theta \right)^2 \cdot (1 + j\eta) \sin^4 \varphi \right],$$

where the symbols are the same as for the thin plate in section 5.2.7.1 but now there are two coincidence frequencies calculated from the stiffness's in direction x and z. The expression above is due to Hansen (1993). However, Heckl basically worked it out in 1960 but not including the term with the loss factor η .

Two basic types of corrugated panels are implemented, the cladding and the “wave” corrugated type as depicted in *Figure 5-20* a) and b). The bending stiffness and the resulting

coincidence frequencies as well as the effective surface mass are calculated from the material properties and the geometry of the panel.

For the bending stiffness of the cladding the expressions due to Cordonnier-Cloarec (1989), cited by Buzzi et al. (2003), is used¹. Similar expressions for the wave-corrugated panel are taken from a book by Timoshenko and Woinowsky-Krieger (1959). To calculate the effective surface density in this case involves finding the length of the sinusoidal “wave”. This is implemented by a Gaussian numerical integration routine.

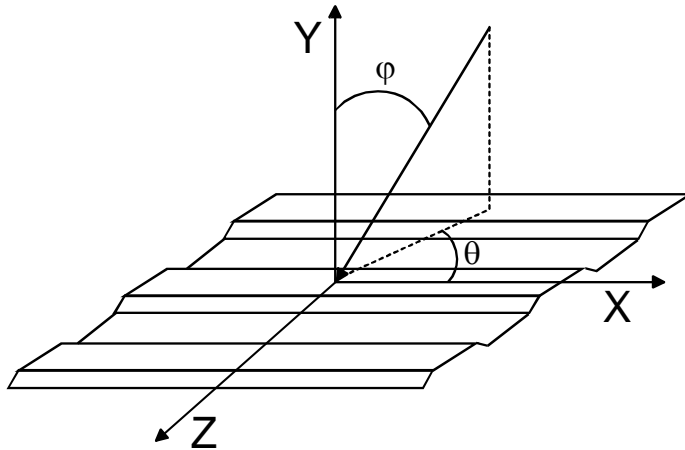


Figure 5-19 Corrugated panel with coordinate system. Incident wave indicated by arrow.

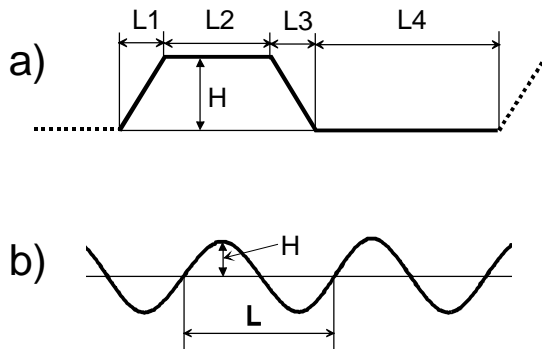


Figure 5-20 Sketch of cross section of corrugated panels.

a) Cladding b) “Wave” corrugated

The properties windows for these two plates are shown in Figure 5-21. Simultaneously with these windows sketches similar to the ones shown in Figure 5-20 will appear to facilitate the input process.

Please observe that the height H of the “wave” includes the thickness of the plate and therefore cannot be set smaller than this thickness, i.e. the plate is flat for H equal to the thickness. For the cladding the height H is zero for the equivalent flat plate.

Furthermore, it should be observed that the azimuth angle θ of the incident wave is now a property for these layers.

¹ It should be observed that the definition of the symbol b , defining the neutral axis, is missing in the paper by Buzzi et al.

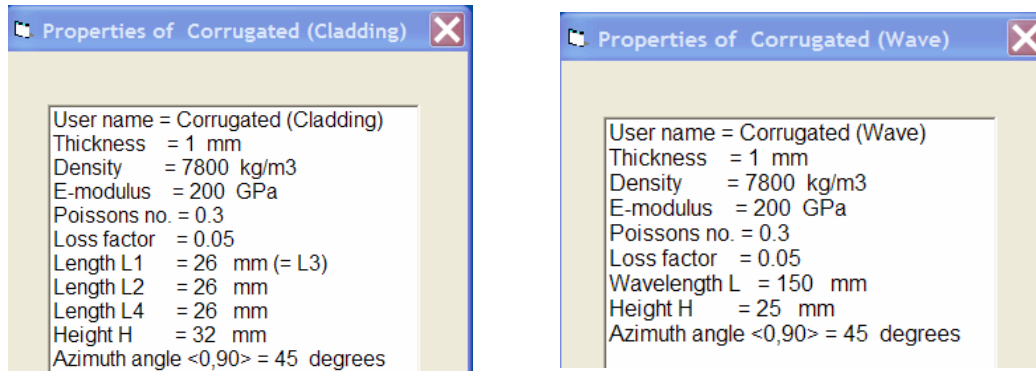


Figure 5-21 The properties windows for the two types of corrugated plates (panels)

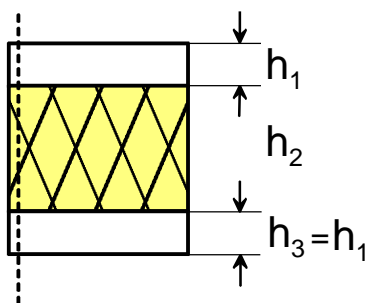
NOTE Combining corrugated plates with other plane layers there will be air cavities between the corrugated plate and the other layers. This is not accounted for in the calculations.

References:

1. Hansen, C.H. (1993) Sound transmission loss of corrugated panels. *Noise Control Eng. J.*, **40**, 187 - 197.
2. Heckl, M. (1960) Untersuchungen an Orthotropen Platten. *Acustica*, **10**, 109 - 115.
3. Buzzi, T, Courné, C, Moulinier, A and Tisseyre, A. (2003) Prediction of the sound reduction index: A modal approach. *Applied Acoustics*, **64**, 793 – 814
4. Timoshenko, S.P. and Woinowsky-Krieger, S. (1959) *Theory of plates and shells*, 2nd Ed., McGraw-Hill, New York.

5.2.7.4 Sandwich

As stated above the sandwich is a special case. The “layer” is actually a combination of three separate layers, a core with two face sheets; see sketch in *Figure 5-22*. The core is an elastic layer described by a 4x4 matrix discussed above; see Section 5.2.7.2. We may, however, include the sandwich panel as one single layer if we are able to find the equivalent wall



impedance Z_W for the total element in the same way as for the single plates. Knowing the wall impedance, the transmission loss may be calculated. Again, there should only be fluid layers directly in contact with this element.

Figure 5-22 Sandwich panel with core and identical face sheets.

The calculation routine is based on a paper by Moore and Lyon, see the reference below, who describe the wave motion of a panel construction with thin face sheets and a thicker and lighter core. The core may be orthotropic but this option is not implemented here. The program presupposes that the core as well as the face sheets is homogeneous and isotropic.

Furthermore the face sheets are considered to be identical. The sandwich panel may in the same way as an elastic layer have symmetric as well as antisymmetric propagating modes,

i.e. there may be thickness deformation of the core (dilatational modes) as well as deformation of the panel without changes in thickness. Both types of modes give rise to coincidence phenomena with normally result in increased sound transmission.

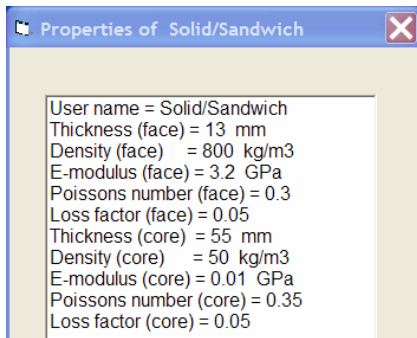


Figure 5-23. The properties window for a sandwich panel with identical face sheets.

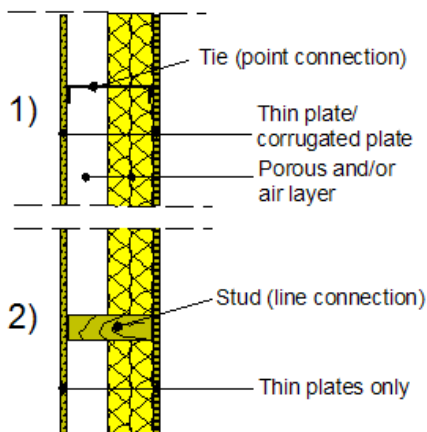
Figure 5-23 shows the window for specifying the parameters of the sandwich panel. The uppermost five lines, indicated with (face), give the parameters for the identical face sheets. The corresponding data for the core are indicated by (core).

Reference:

Moore, J. A. and Lyon, R. H. (1991) Sound transmission loss characteristics of sandwich panel constructions. *J. Acoust. Soc. Am.* **89**(2), 777 - 791.

5.2.8 Structural bridges

These layers simulate structural connections, either in the form of studs (line connections) or as “ties” (point-like) between the outer plate layers in a double construction. It is assumed that these bridges are massless but the programs offers the choice of assuming that they are either



infinitely stiff or have a given flexibility. In the first case, they may simulate wooden studs whereas in the latter case, flexible types made of steel are simulated. At present, there will be strict limitations as to the allowed configurations which may be used when including these bridges. Figure 5-24 shows the two basic configurations which are allowed. It should be noted that only thin plates (see Remark below) or corrugated plates may be used as outer layers. For combinations with studs, corrugated plates cannot be used. See also remarks below.

Figure 5-24 Configurations allowed when including the layer named Structural bridges.

REMARK It should be remembered; see the last paragraph in Section 5.2.7.2, that for sound transmission calculations thin plate theory may be applied to quite massive plates or walls. This means that the effect of adding so-called acoustical linings to a heavy wall may be estimated using the configurations shown above.

5.2.8.1 Stiff structural bridges

The influence of the bridges is implemented based on an idea put forward by Sharp, see reference [1] below. He shows that the resulting diffuse sound reduction index due to the action of the bridges may be expressed as

$$R = R_{NB} - \Delta R_B$$

where R_{NB} is the reduction index without the bridges and ΔR_B is a correction term due to the action of the bridges. The latter term is expressed as

$$\Delta R_B = 10 \cdot \lg\left(1 + \frac{W_B}{W_{NB}}\right).$$

Here W_{NB} is the sound power radiated from the second plate (plate no. 2) without the bridges and W_B is the extra sound power radiated from this plate due to the action of the bridges. The ratio of these, assumed uncorrelated, powers may be expressed as

$$\frac{W_B}{W_{NB}} = n \cdot \sigma_B \cdot \left| \frac{Z_{B1}}{Z_{B1} + Z_{B2}} \right|^2 \cdot \left\langle \left| \frac{v_1}{v_2} \right|^2 \right\rangle$$

Here σ_B is the radiation factor (or radiation efficiency) of the second plate driven by one of the number n bridges acting over the partition area S . (Please note that this radiation factor is different from the one commonly used for plates, which is based on the time- and space-averaged velocity). The Z_B 's are the input impedances of the respective plates seen from bridge. Finally, the last term is the squared velocity ratio of the two plates without the action of the bridges, averaged over the angle of incidence, the average indicated by the brackets $\langle \rangle$.

In reference [1] approximate expressions for the above quantities are used, especially for the last term. However, this term may directly be derived from the final matrix for the system. Expressions for the other quantities may be found in the literature, see e.g. reference [2, 3]. For corrugated plates, expression for the radiation factor (point-drive or ties only) is taken from reference [4].

The properties window for the stiff structural bridges is given in *Figure 5-25*. For information, *Figure 5-24* will appear next to this window. As apparent from the properties window one may choose between rigid point connections (ties) and line connections (studs). Choosing ties, by putting a zero (0) in the second line, the area per tie (the wall area divided by the number of point connectors) must be specified and the information on studs is irrelevant. For studs, putting a one (1) in the second line, the c-c distance must be specified. It

should be noted that only thin plate layers can take part, also, for corrugated plates only point connections apply.

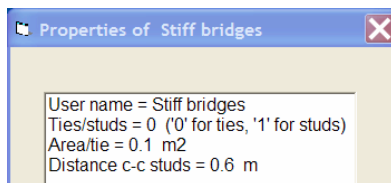


Figure 5-25 The property window for stiff structural bridges.

I might, however, be difficult to decide, even for wooden studs, whether line connections or a series of point connections should be chosen. Experience shows, see e.g. references [5, 6], that the spacing of the screws (or nails) attaching the plates to the studs is important making this choice. As a rule of thumb: if the distance between the screws is less

than half the wavelength of the bending wavelength in the plate, studs should be the choice. This will also give a conservative estimate of the sound reduction index.

As pointed out above, only thin plates are allowed. However, experience shows that thin plate theory may be applied outside the common limit, demanding that the wavelength in the plate should be more than six times the plate thickness. An example is shown in Annex F where measured and predicted results are given for a lightweight concrete wall where a so-called acoustical lining is attached, 13 mm plasterboard connected with studs to the concrete wall, the cavity being filled with mineral wool. As the procedure, correcting for the effect of the sound bridges, is an approximation only, the sound reduction index may depend on direction for strongly non-symmetrical constructions. Preferably, the heaviest plate should be placed as the first layer.

References:

- [1] Sharp, B.H. (1978) Prediction methods for the sound transmission of building elements. *Noise Control Eng.*, 11, 53–63.
- [2] Vigran, T.E. (2008) *Building Acoustics*, Taylor & Francis, London and New York.
- [3] Vigran, T.E. (2010) Sound transmission in multilayered structures – Introducing finite structural connections in the transfer matrix method, *Applied Acoustics*, 71, 39–44.
- [4] Heckl, M. (1960) Untersuchungen an Orthotropen Platten, *Acustica*, 10, 109–115.
- [5] Craik, R.J.M. and Smith, R.S. (2000) Sound transmission through double leaf lightweight partitions, part I: airborne sound. *Applied Acoustics*, 61, 223–245.
- [6] V. Hongisto, M. Lindgren and R. Helenius (2002) *Acta Acustica united with Acustica*, 88, 904–923. Sound insulation of double walls – An experimental study.

5.2.8.2 Flexible bridges

Concerning flexible bridges, simulated results have been compared with measurement results only in the case of C-channel metal studs having a cross-sectional shape as sketched for tie connections in *Figure 5-24*; see also reference [1] below. However, the possibility of including flexible tie connections has been included based on a similar procedure as for studs.

The general frequency dependence of the C-type metal studs simulated is based on the work cited in reference [2] below. By numerical modelling, metal studs of different cross sections were tested in three types of lightweight double walls. The equivalent stiffness function of the C-type stud (denoted TC in [2]), which is approximated by a smooth curve, is used in this case. The function is depicted in *Figure G-1* in Annex G. As seen from this figure, the stiffness is relatively constant at low frequencies, a stiffness which represents the input parameter to the stud stiffness per unit length in the property window; see *Figure 5-26* below. The default value (1 MN/m^2) is assumed to apply for C-type studs of width (cavity depth) 60–90 mm and material thickness (0.55 ± 0.05) mm. Furthermore, changing this stiffness value by e.g. a factor of two, the stiffness for all frequencies is multiplied by the same factor.

An example, comparing measured and predicted results for the sound reduction index of a double-leaf lightweight wall with plasterboards, is shown in *Figure G-2* in Annex G. Also shown here are predicted results assuming that the studs in question are either not present or being infinitely stiff.

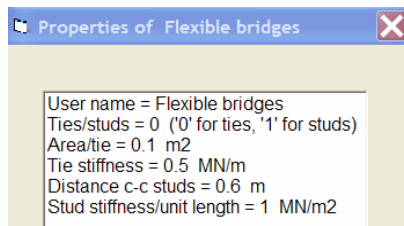


Figure 5-26 The property window for flexible structural connections (bridges)

References

- [1] Vigran T. E. (2010) Sound insulation of double-leaf walls – Allowing for studs of finite stiffness in a transfer matrix scheme. *Applied Acoustics* 71, 616–621.
- [2] Poblet-Puig J, Rodriguez-Ferran A, Guigou-Carter C, Villot M. (2009) The role of studs in the sound transmission of double walls. *Acta Acustica/ Acustica* 95, 555–567.

5.3 THE FREQUENCY MENU

The submenus have the following items:

- Frequency range
- Linear scale
- Logarithmic scale

Clicking on any of these items starts a new calculation.

Submenu	Shortcut	Description
Frequency range	Ctrl F	Opens up a new window to specify the frequency range of the calculations including the number (max. 500) of frequency lines used, see <i>Figure 5-27</i> .
Linear scale	None	The frequency is incremented linearly
Logarithmic scale	None	The frequency is incremented logarithmically. This option is automatically chosen when calculating mean values in one-third-octave bands; see calculation options under Section 4.1.

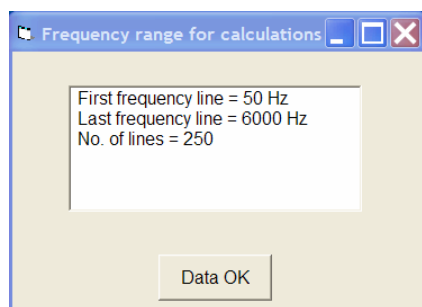


Figure 5-27 Window for setting the frequency range and number of lines used in the calculations

The frequency range used in the calculations is always specified by the first and the last frequency line in addition to the total number of lines inside this range. When calculating mean values in one-third-octave bands one should preferably set the first frequency line equal to or lower than the lower cut-off frequency of the first frequency band of interest. Conversely, the last frequency line should be equal to or higher than the upper cut-off frequency of the last band of interest.

5.4 THE SOUND INCIDENCE MENU

The submenus have the following items:

- Angle
- Diffuse
- Reverberation room

Clicking on any of these items starts a new calculation.

Submenu	Shortcut	Description
Angle	Ctrl V	Opens up a window for specification of the plane wave angle of incidence (between 0 and 90 degrees). Zero degrees signify normal incidence.
Diffuse	Ctrl D	Calculates a mean value for all angles of incidence. More details concerning this calculation are given below.
Reverberation room	Ctrl K	Calculates an estimate of the absorption coefficient measured for the actual absorbent configuration in a standardised reverberation room test. An option to estimate the weighted coefficient α_w is included; see the description under Section 5.4.2. The specimen is assumed to have a square shape and choosing this option brings up a window for input of the length of the side of the square. The default value is 3.162 meter giving approximately an area of 10 m ² .

When choosing the "Diffuse" option, mean values for the absorption coefficient and the sound reduction index are calculated, the latter one only if relevant. Mean values are not calculated for the impedance. Furthermore, the reverberation room option only applies to the case of absorption coefficients. Some details concerning the calculation of these mean values are given under the Section 5.4.1.

5.4.1 Statistical absorption and transmission coefficients

Choosing the item "Diffuse" a statistical absorption coefficient α_{stat} is calculated using the expression

$$\alpha_{\text{stat}} = 2 \int_0^{\pi/2} \alpha(\varphi) \sin \varphi \cos \varphi d\varphi,$$

where $\alpha(\varphi)$ is the absorption coefficient with the incident angle φ . If relevant for the actual configuration, i.e. the layer HARD WALL (Rigid backing) is not included, a mean transmission coefficient τ_{stat} is calculated in the same way and the mean sound reduction index R in dB is displayed. In this case, however, the transmission coefficient for the infinite size structure is corrected applying a so called spatial windowing technique before carrying out the integration; see explanation under menu "Sample size", Section 5.5. This procedure replaces the simple one used in earlier versions of the program, i.e. setting the upper limit of

the integration to approximately 80 degrees to get a better fit between measured and calculated results. In each case the integral is solved numerically using a Gaussian routine.

The procedure outlined above applies for all configurations not including any of the corrugated plate layers. In such a case a two-dimensional integration is performed, i.e. the azimuth angle θ for the sound incidence is integrated over as well. For information, see *Figure 5-19*.

With the menu item "Reverberation room" integration over the angle of incidence is also performed. In this case, however, the limited size of the absorbent is taken into account. Due to diffraction effects the effective "acoustical size" may become larger than the actual geometrical size of the absorber. As a result of this so-called edge effect the absorption coefficient may become larger than 1.0.

Thomasson, see the reference below, have shown that we may write

$$\alpha_{\text{stat}} = \frac{4 \operatorname{Re}\{Z_n\}}{\pi} \int_0^{\pi/2} \int_0^{2\pi} \frac{\sin \varphi}{|Z_n + Z_f|^2} d\varphi d\theta ,$$

where Z_n is the normalised input impedance of the absorber (normalised to $\rho_0 c_0$). The impedance Z_f is by Thomasson called "field impedance" which is dependent on the shape and dimensions of the absorber and also on frequency and the angle of incidence. In general the sound incidence must be specified by the angle of incidence φ referred to the normal and to the azimuth angle θ as well.

The calculations in the program presuppose a square specimen. Please observe that the formula above applies to *locally reacting* materials. In the case of mineral wool type of porous materials the calculations have shown to be fairly accurate. Applied to bulk reacting absorbers as resonance absorbers where the airspace is not subdivided (into cassettes) the accuracy is not asserted. Probably the edge effect is a little overestimated.

Reference:

S.-I. Thomasson (1980), On the absorption coefficient, *Acustica* **44**, 265 - 273.

5.4.2 Weighted sound absorption coefficient

The weighted sound absorption coefficient α_w according to ISO 11654 may be estimated, see the reference below. This applies when using the menu item "Reverberation room" and the option one-third-octave band is set. A button with the caption "Alpha W" will then appear at the bottom right of the graphical picture. Clicking the button will run a calculation and the caption will show the estimated value α_w together with the proper shape indicators L, M or H. This calculation presuppose that the side length of the absorber is in the range 3.16 – 3.46 meter, i.e. the area is between 10 and 12 m² as given in the measurement test procedure in ISO 354, see below. The default value of this side length is 3.162 meter.

Calculation of α_w is based on standard reverberation room measurement results of the sound absorption coefficient in one-third-octave bands. The measurement procedure is described in the standard ISO 354; a reference is given below. From these results practical sound absorption coefficients α_{pi} in the octave bands 250, 500, 1000, 2000 and 4000 Hz are calculated according to certain rounding rules. These data are then compared with a reference curve having the following values in the octave bands listed above: 0.8, 1.0, 1.0, 1.0 and 0.9. This reference curve is shifted in steps of 0.05 until the sum of the unfavourable deviations is less than or equal to 0.1. An unfavourable deviation occurs when at any octave band the measured value is less than the reference value. Only deviations in the unfavourable direction

are counted. Finally, the weighted sound absorption coefficient is defined as the value of the shifted reference curve at 500 Hz.

Shape indicators shall be added to α_w (in parentheses) if the practical sound absorption coefficient exceeds the shifted reference curve by more than 0.25, using the letter L if excess absorption occurs at 250 Hz, M if it occurs at 500 or 1000 Hz and H if it occurs at 2000 or 4000 Hz.

An example on a calculation is shown in *Figure 5-28* where the button "Alpha W" has been clicked on, see lower right corner.

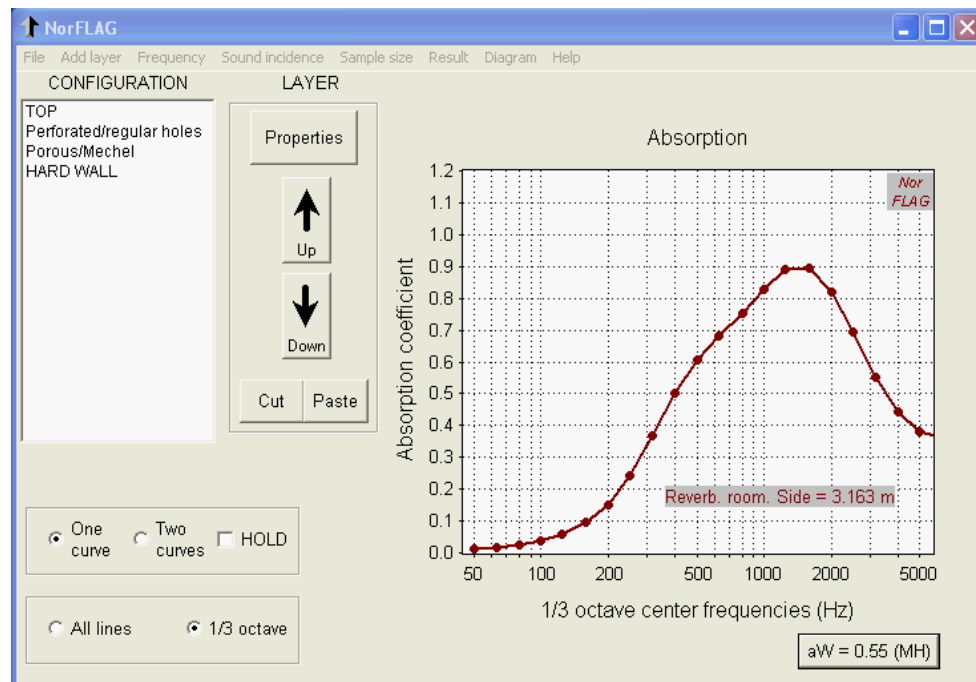


Figure 5-28 The main window showing a calculated weighted sound absorption coefficient α_w and shape indicators. The parameters are the same as used in Figure 4-4, except for the thickness of the porous material which is reduced to 25 mm.

Reference:

1. ISO 11654:1997 Acoustics -- Sound absorbers for use in buildings. Rating of sound absorption.
2. ISO 354:2003 Acoustics -- Measurement of sound absorption in a reverberation room

5.4.3 Weighted sound reduction index

The weighted sound reduction index $R_w(C; C_{tr})$, where C and C_{tr} are the spectral adaptation terms according to ISO 717-1, may be estimated, see the reference below. This applies when using the menu item "Diffuse" and the option one-third-octave band is set. A button with the caption "R-weighted" will then appear at the bottom right of the graphical picture (In the same position as the button for α_w ; see *Figure 5-28*). Clicking on the button a calculation will run and the caption will show the estimated value $R_w(C; C_{tr})$ provided the frequency range is sufficiently large, see *Figure 4-6*. The frequency range used for these adaptation terms are the

one-third-octave bands 100 – 3150 Hz. It should be noted that the standard ISO 717-1 also contains an option for calculating adaptation terms for an enlarged frequency range; terms denoted $C_{50-3150}$, $C_{50-5000}$, $C_{tr, 50-3150}$, $C_{tr, 50-5000}$ and $C_{tr, 100-5000}$. These terms are presently not implemented in the program.

Calculation of R_w is normally based on laboratory measurement of the sound reduction index R in one-third-octave bands from 100 Hz to 3150 Hz. The measurement procedure is described in the standard ISO 10140 part 2 (formerly ISO 140 part 3); a reference is given below. The measured data are rounded to one decimal and compared to a reference curve. This reference curve is shifted in steps of 1 dB until the sum of the unfavourable deviations is less than or equal to 32 dB. An unfavourable deviation occurs when at any one-third-octave band the measured value is less than the reference value. Only deviations in the unfavourable direction are counted. Finally, the weighted sound reduction index is defined as the value of the shifted reference curve at 500 Hz.

Following the calculation of R_w the spectral adaptation terms C and C_{tr} are calculated according to the procedure given in Section 4.5 in ISO 717-1, using the proper 1/3 octave sound level spectra in Table 4 in this standard.

It should be observed that the uncertainty of data for R_w based on calculated data, rather than measured ones, could be large. However, due to the simulation of a finite size specimen by the spatial windowing technique, see section 5.5, together with the possibility to introduce mechanical connections between layers, as described in section 5.2.8, the accuracy of R_w should be greatly improved compared with earlier versions of the program.

Several other programs are available to predict the weighted sound reduction index and adaptation terms of partitions. Kurra; see reference 3 below, has compared predictions from three programs, not including NorFlag, on altogether 65 buildings elements, single and multi-layered. The multi-layered ones are, however, all without structural connections. It is easily demonstrated that NorFlag compares favourably.

Reference:

1. ISO 717-1: 2013 Acoustics -- Rating of sound insulation in buildings and of building elements. Part 1: Airborne sound insulation
2. ISO 10140-2: 2010 Acoustics -- Measurement of sound insulation in buildings and of building elements. Part 3: Laboratory measurements of airborne sound insulation of building elements.
3. S. Kurra (2012). Comparison of the models predicting sound insulation values of multilayered building elements. *Applied Acoustics* **73**, 575-589.

5.5 THE SAMPLE SIZE MENU

This menu gives the means to specify the specimen area when simulating measurement of the absorption coefficient in a reverberation room or when simulating measurement of the sound reduction index in a laboratory transmission suite, the latter by the so-called spatial windowing technique. The submenus is named as follows

- Reverberation room
- Transmission suite

Clicking on these items brings up a window to input, either the side length (m) of the sample in the reverberation room or the area (m²) of the specimen for sound transmission calculation.

Submenu	Shortcut	Description
Reverberation room	None	Opens up a window for specification of the side length of a square specimen in the reverberation room. The default value is 3.163 meter, giving an area of approximately 10 m ² .
Transmission suite	None	Opens up a window for specification of the area of the sample for calculating the sound reduction index of the given configuration. The default value is 10 m ² . See explanation below on the background for introducing this feature.

The transmission suite area (or “window” area) is introduced to take account of a finite size as compared with the infinite sample size inherent in the normal transfer matrix calculations. The procedure is based on the work of Villot *et al.*, see references [1, 2] below, where the technique is named “spatial windowing”. The idea is to simulate a finite size rectangular area ($L_x \cdot L_y$) by placing a “window” of this size either on one or both sides of the otherwise infinite size structure, thereby making it possible to modify the incident wave field and the radiation from the structure. The effect is to obtain more realistic values for the sound reduction index, especially for multi-layered structures. Formerly, NorFlag applied the common method of limiting the diffuse value integration to 78–80 degrees to obtain better fit to experimental data. The windowing technique implies performing two double integrations for each angle of incidence. This may lead to quite long computation times, especially for corrugated plates where the average is taken over the azimuth angle as well. A simplified procedure is therefore used, see reference [3], based on using $(L_x \cdot L_y)^{1/2}$ as the characteristic dimension in the calculations. An example is shown in Annex E.

- [1] Villot, M., Guigou, C. and Gagliardini, L. (2001) Predicting the acoustical radiation of finite size multi-layered structures by applying spatial windowing on infinite structures. *J. Sound and Vibration*, 245, 433–455.
- [2] M. Villot and C. Guigou-Carter (2005) Using spatial windowing to take the finite size of plane structures into account in sound transmission. NOVEM, Biarritz, France.
- [3] Vigran, T.E. (2009) Predicting the sound transmission index of finite size specimen by a simplified windowing technique. *J. Sound and Vibration*, 325, 507–512.

5.6 THE RESULT MENU

The menu gives the choice on which calculated result should be displayed, i.e.

- Absorption coefficient
- Input impedance
- Sound reduction index
- Duct attenuation

None of these choices calls up the calculation procedure because all relevant data are calculated simultaneously. For the duct attenuation two sub-items are available, Rectangular and Circular (cross section). For each of these there are the sub items Show (results) and Calculate. The latter recalculates if certain conditions are met, see the table below. More details on duct attenuation are given under the Section 6.

Submenu			Short cut	Description
Absorption coefficient			Ctrl A	Display the chosen values for the absorption coefficient, i.e. the coefficient for a given angle of incidence, a mean value in a diffuse field or an estimate from a reverberation room.
Impedance			Ctrl I	Display the real and imaginary part of the normalised input impedance for a given angle of incidence. The reference impedance Z_0 is 415 Pa·s/m.
Sound reduction index			Ctrl R	Display the chosen values for the sound reduction index, either for a given angle of incidence or a mean value in a diffuse field. In the latter case the upper limit of integration is 80 degrees.
Duct attenuation	Rectangular	Show	None	Display the result for the duct attenuation in dB/m if the following conditions are set for the layer configuration <ul style="list-style-type: none"> • At least one porous layer is present • The HARD WALL is included • The incidence angle is set to zero degrees
		Calculate	None	Provided the above conditions are fulfilled this choice brings up a window to input the half-width h of the air duct, see <i>Figure 6-1</i> , the default value is 150 mm. Performs a recalculation and displays the result. ¹
	Circular	Show	None	As above for the rectangular duct
		Calculate	None	As above for the rectangular duct, bringing up a window to input the duct radius h , see sketch to the right in <i>Figure 6-1</i> .

¹ A maximum obtainable number of dB's attenuation per length of duct related to the cross dimension h is often used as a "rule of thumb" in the design of silencers. This limit will be indicated by a dotted line in the graph.

5.7 THE DIAGRAM MENU

The menu offers the choice of changing the values on the axes of the diagram. No new calculations are performed. The choices are the following:

- First frequency
- Last frequency
- Y minimum
- Y maximum

Submenu	Shortcut	Description
First frequency	None	Opens up a window to specify the first frequency marking on the abscissa. The default value is 45 Hz.
Last frequency	None	Opens up a window to specify the last frequency marking on the abscissa. The default value is 5700 Hz.
Y minimum	None	Opens up a window to specify the minimum value for the ordinate. The default value is zero except when displaying the impedance where the value is -10.
Y maximum	None	Opens up a window to specify the maximum value for the ordinate. The default values are 1.2, 10.0 and 50.0 for the absorption coefficient, the impedance and the sound reduction index, respectively. The last value also applies to the duct attenuation.

5.8 THE HELP MENU

The choices are:

- Opening the full manual (pdf-file)
- Opening a material property list (pdf-file)
- Information on NorFLAG

Submenu	Shortcut	Description
Manual (pdf-file)	Ctrl H	Opens up this help file in pdf-format. The program to read this file, Adobe Reader or a similar program, must be installed.
Properties of materials	Ctrl M	Opens up separately Annex B in this help file.
About NorFLAG	None	Displays an information window on NorFLAG

6 ATTENUATION IN DUCTS (SILENCERS)

Calculation of the attenuation of silencers is not a part of the general transfer matrix scheme used in NorFLAG. Knowing the input impedance of a certain configuration of layers one may however estimate the attenuation applying such a lining to a duct wall. The literature on the subject is extensive and procedures exist to calculate the attenuation of silencers of almost any cross section and also of finite length. The latter implies a complex mode matching technique to match the modal pattern in both the input and output duct to the modal pattern in the lined part of the duct. For a calculation and a review of procedures for handling finite length silencers see e.g. a paper by Kirby (2001), see the full reference below.

The implementations in the program are restricted to the calculation on either a rectangular symmetrical silencer (of infinite length) or on a circular duct silencer; see *Figure 6-1*. Approximate formulas given by Frommhold and Mechel (1990), see the reference below, is used. Furthermore, only the formulas dealing with locally reacting linings are implemented; i.e. we assume that there is no sound propagation along the duct inside the lining itself. In practice this implies that in case of a porous lining material the flow resistivity must be high enough or there must be hard partitions (cassettes) to prevent the sound propagation inside the lining itself. The same restriction applies of course to a resonant lining, i.e. a Helmholtz resonator type of lining.

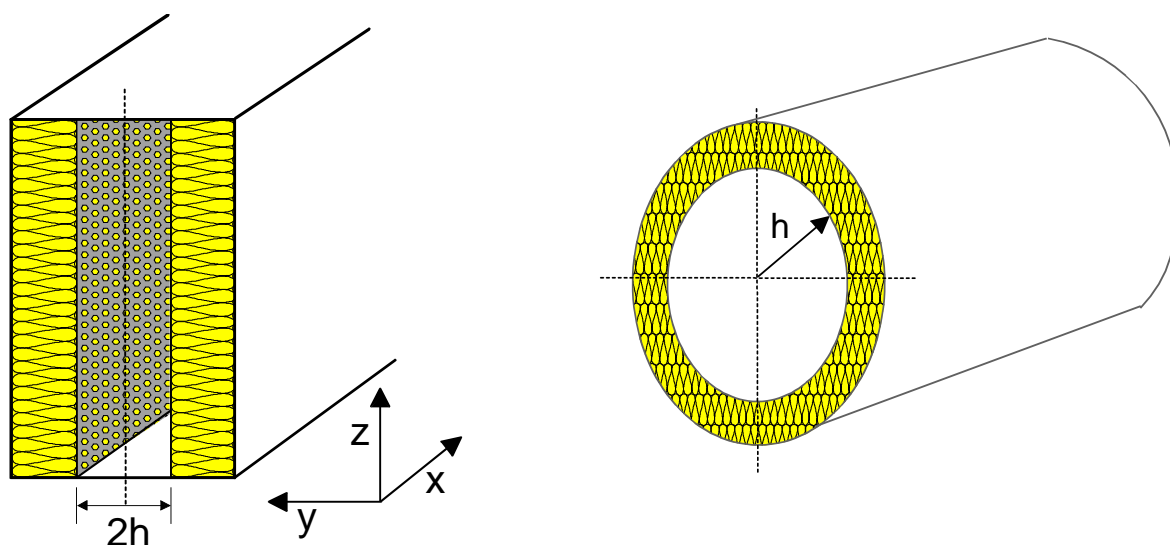


Figure 6-1. Rectangular and circular duct silencers

The attenuation in dB per meter of lined duct is calculated by approximate solutions of the wave equation for the sound field in the air duct, see details below. Partly because the approximations will be poor in the neighbourhood of critical branch points, some restrictions are imposed in the program. No calculations are performed if the following conditions are not met:

- At least one porous layer must be present in the lining
- The HARD WALL must be present (simulates the duct outer wall)
- The sound incidence angle must be set to zero degrees

Also please observe that the attenuation always applies to the least attenuated mode, which means that the estimate generally is a conservative one. However, one may experience quite large attenuation rates in smaller frequency ranges, may be 8–10 dB per length of duct equal to the half-width (or radius) h . However, in practice there will always be other sound transmission mechanisms coming into play when the primary sound transmission path is sufficiently attenuated.

Such mechanisms may be vibration transmission along the duct walls whereas another is the so-called “break-out” phenomenon, i.e. sound transmission directly out through the duct wall and into the surroundings. This sound energy may subsequently have the possibility to re-enter (“break-in”) another part of the duct. Flexible connections in the ductwork are certainly a weak point in this respect. Designing a single silencer having a total attenuation in excess of say 40–50 dB is then very difficult. Other “rules of thumb” concerning the maximum attainable attenuation are also in existence. One of these is to set 3dB/half-width as a maximum attenuation limit for a rectangular duct lined on two sides. This limit is therefore indicated when performing these calculations; see under Section 5.6. A square duct with linings on all walls or the equivalent circular duct (diameter $2 \cdot h$ inside the lining) will approximately give twice the attenuation.

6.1 RECTANGULAR DUCT WITH LINING ON TWO WALLS

With the assumptions given above and furthermore that the sound field in any cross section is the same in the z -direction, the equation for the complex wave number k_y in the crosswise direction may be written

$$(k_y \cdot h) \cdot \operatorname{tg}(k_y \cdot h) = j \frac{k_0 \cdot h}{Z_{n0}},$$

where $2 \cdot h$ is the width (or depth) of the air channel and Z_{n0} is the normalised input impedance of the lining at normal incidence (zero degree incidence angle). Solving this equation for k_y we may from the total wave number k_0 find the complex wave number k_x in the direction of flow. For the latter, which will give us the attenuation, we may write

$$k_x = \operatorname{Re}\{k_x\} + j \cdot \operatorname{Im}\{k_x\} = \sqrt{k_0^2 - k_y^2},$$

where $\operatorname{Re}\{\}$ and $\operatorname{Im}\{\}$ signify the real and imaginary part of the wave number. The attenuation for a length ℓ of duct is then given by

$$\Delta L = 20 \lg(e) \cdot \operatorname{Im}\{k_x\} \cdot \ell \quad (\text{dB}).$$

(Using the complex propagation coefficient Γ instead of the complex wave number k the real part of Γ must be used in the last equation).

Frommhold and Mechel (1990) express the equation to be solved for k_y as

$$\sqrt{E} \cdot \operatorname{tg}(\sqrt{E}) = j \cdot U,$$

and they use an expansion of the left-hand side by a so-called method of continued fractions to arrive at polynomial approximations of the equation of various orders. We shall use the quadratic approximation given in the equation (42) and (43) in the paper, which is

$$E_{1,2} = \frac{(78.94 - j \cdot 5.43) + jU(34.47 - j \cdot 2.2) \pm \sqrt{\quad}}{(16.1 - j \cdot 1.11) + 2jU},$$

where

$$\sqrt{\quad} = \sqrt{(6203 - j \cdot 857) + jU(2887.3 - j \cdot 372) + (jU)^2(867.4 - j \cdot 130)}.$$

The calculation in the program always uses the solution giving the least attenuation.

6.2 CIRCULAR DUCT

For a duct of circular cross section the analogue expression to be solved for the complex wave number k_y is

$$\frac{\sqrt{E} J_1(\sqrt{E})}{J_0(\sqrt{E})} = j \cdot U ,$$

where J denote Bessel functions of the first kind. A quadratic approximation is given in equation (48) in the paper by Frommhold and Mechel, albeit with a small misprint. The correct formula should read

$$E = \frac{96 + 36jU \pm \sqrt{9216 + 2304jU + 912(jU)^2}}{12 + jU}$$

Important note: The input impedance calculated by the NorFlag procedures, which applies to plane surfaces, is strictly not applicable to the curved surface of this kind of duct. It leads to a slightly less attenuation than when using the correct input impedance of the curved wall. This is illustrated in *Figure 6-2* showing the attenuation in a duct of two different diameters where the lining is a 100 mm thick porous absorbent. To compensate for this effect and arrive at a better fit, Mechel (1998) (see reference below) suggests that, in calculations using the plane alternative, the thickness should be set to

$$d_{\text{plane}} = d_{\text{circular}} \left(1 + \frac{d_{\text{circular}}}{3h}\right),$$

where h is the radius of the duct.

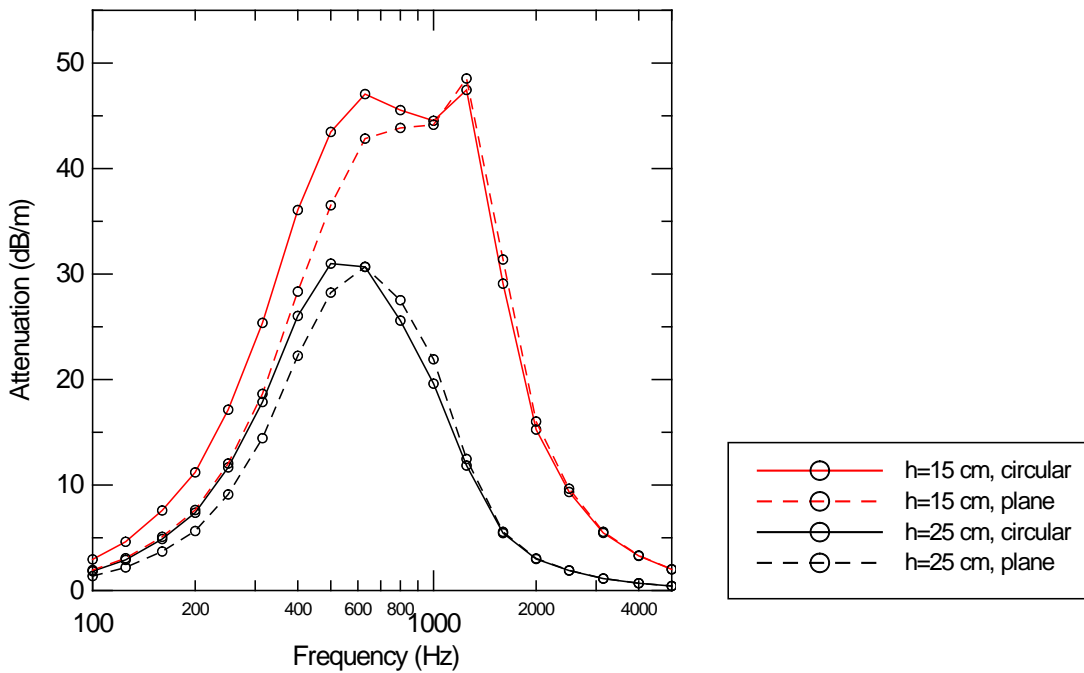


Figure 6-2 Attenuation in circular ducts. Calculations assuming circular vs. plane duct wall. Mechel model of porous material of thickness 100 mm with flow resistivity of 10 kPa·s/m².

References:

1. Frommhold, W. and Mechel, F.P. (1990) Simplified methods to calculate the attenuation of silencers, *J. Sound Vib.* **141**(1), 103–125.
2. Mechel, F.P. (1998) Modal solutions in circular and annular ducts with locally or bulk reacting linings. *Acustica/Acta Acustica* **84**, 201–222.
3. Kirby, R. (2001) Simplified techniques for predicting the transmission loss of a circular dissipative silencer, *J. Sound Vib.* **243**(3), 403–426.

ANNEX A. CONFIGURATION FILE

The configuration file will contain the complete user set-up, i.e. the layer configuration together with the relevant parameters, either specified by the user or the default ones. The file name is given by the user but the file gets the extension ".lag". One line of heading text is also asked for before the file is saved; see the first line in the example below.

The file is, however, a plain text-file (ASCII) that may easily be edited by the user in an ordinary text editor, e.g. Microsoft Notepad or similar. *Such an editing will be necessary if one wants to use a configuration file from earlier versions of WinFLAG.* New types of layers introduced in WinFLAG Version 2.0 onwards necessitate a use of a total of ten parameters whereas the former version had eight only. A later introduction (in version 2.3) of a finite sample size for transmission calculations also demanded an additional quantity ("Window area").

The following lines give an example of a configuration file where the print in **red colour** has to be added to the old configuration files. Only the numbers are important for reading the file into the program, the text between the quotation marks is just for explanation and could be an empty string.

Example:

```
"4-layer sample configuration"
50,"First frequency"
6000,"Last frequency"
250,"No. of lines"
1,"Identifier for the scale"
0," Identifier for 1/3 octave"
0,"Angle"
2,"Identifier for incidence"
3.163,"Side length"
10,"Window area"
150,"Duct half-width or radius"
4,"No. of layers"
18,"Porous facing"
3,"Porous/Mechel"
1,"Air"
11,"HARD WALL"
1,.25,200,70,1,0,0,0,0,0
50,10,95,0,0,0,0,0,0,0
50,0,0,0,0,0,0,0,0,0
0,0,0,0,0,0,0,0,0,0
```

ANNEX B. PROPERTIES OF MATERIALS

The table, together with the graph below, is intended to give an estimate of some important material data in case data for the product is not available from the producer. The data has been collected from various sources and the conditions for the measurements are not always clear. As for the table, the modulus of elasticity (Young's modulus) should for acoustic purposes be tested under dynamic conditions. Most of the data given here is believed to apply under such conditions, but there may be exceptions where it has been tested under static conditions only. Furthermore, the loss factor only concerns the internal loss in the material and the data should only be considered as a rough estimate. One should be aware that the total loss factor of a specimen is not only very sensitive to the mounting conditions but may also vary with frequency.

Material	Density kg/m ³	Modulus of elasticity 10 ⁹ Pa	Poisson's ratio	Loss factor (internal) 10 ⁻³
Metal, glass etc.				
Aluminium	2700	66–72	0.33–0.34	~ 0.1
Copper	8900	110–120	0.35–0.36	~ 0.2
Magnesium	1750	42–45	~ 0.35	
Steel	7700–7800	190–210	0.28–0.31	~ 0.1
Glass	2300–2600	50–65	-	0.6–2.0
Plexiglas	1150	3.8		2–4
Concrete	2300	32–40	0.15–0.2	4–8
Concrete (reinforced)	2400	33–45	0.15–0.2	10–50
Concrete (lightweight aggregate)	1300	3.8	~ 0.2	10–20
Concrete (autoclaved aerated)	400–600	1.0–2.5	~ 0.2	10–20
Panel materials				
Plywood (fir, spruce)	500–600	8–10		10–30
Plywood (birch)	650–700	9–10		10–30
Fibre board (pressed, 5 – 10 mm)	700–950	2–4		10–30
Gypsum board (9 – 13 mm)	800–900	4.1	~ 0.3	10–15
Wooden chipboard	650–800	3.8	~ 0.2	10–30
Mineral wool				
Rock wool ¹⁾	110–135	0.00025–0.00030 ²⁾		
Glass wool ¹⁾	~ 125	0.00011–0.00013 ²⁾		
Plastic materials:				
PVC (hard)	1380–1550	2–3		20–40
Polystyrene	980–1110	1.5–3.9		
Polystyrene (expanded)	10–20	0.0003–0.003		
Polyurethane (foam)	33–72	0.007–0.019	~ 0.4	

¹⁾ High density types intended for vibration isolation, sandwich element etc. ²⁾ At 2 kPa static load

A graph is presented below giving mean values for the flow resistivity of two common types of mineral wool, rock wool and glass wool, indicated on the curves with the letter R and G. Again; the data from the producer should be used if available.

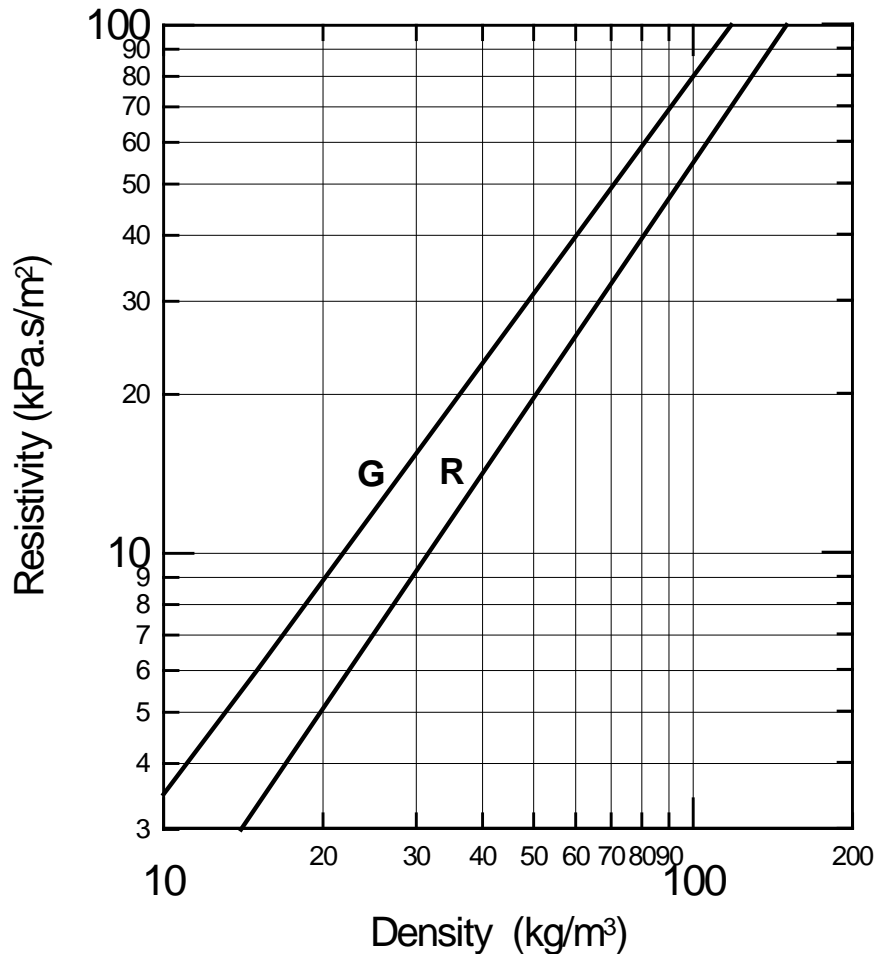


Figure B-1 Flow resistivity for mineral wool of type rock wool and glass wool, curves marked R and G. (typical data for products used in Norway)

Note The flow resistivity of fibrous absorbents is highly dependent on the diameter of the fibres. Empirical relationship between the resistivity, fibre diameter and the density may be found in the reference below.

Reference

Beranek, L.L and Vér, I.L (Editors) (1992) Noise and Vibration Control Engineering, Chapter 8: Sound-absorbing Materials and Sound Absorbers. John Wiley & Sons, Inc., New York.

ANNEX C. MEASUREMENT AND CALCULATION ON A MICROPERFORATED MEMBRANE

In WinFLAG version 1.0 the density of the microperforated layer was listed as a property but actually not used. From version 2.0 onwards the mass impedance is included in the calculation. This is due to the use of thin microperforated plastic foils or membranes where the mass will be of much greater importance than for microperforated metal plates. An example on measurement and calculations on such membranes is shown in *Figure C-1* below. The data is reproduced from the reference cited below and plotted together with calculated results using WinFLAG 2.0.

According to the reference the thickness of the foil is 0.11 mm and has a weight 0.14 kg/m^2 . The diameter of the holes is 0.2 mm and the percentage perforation is 0.79 %. The foil is mounted against a rigid wall at a distance (airspace) of 100 mm.

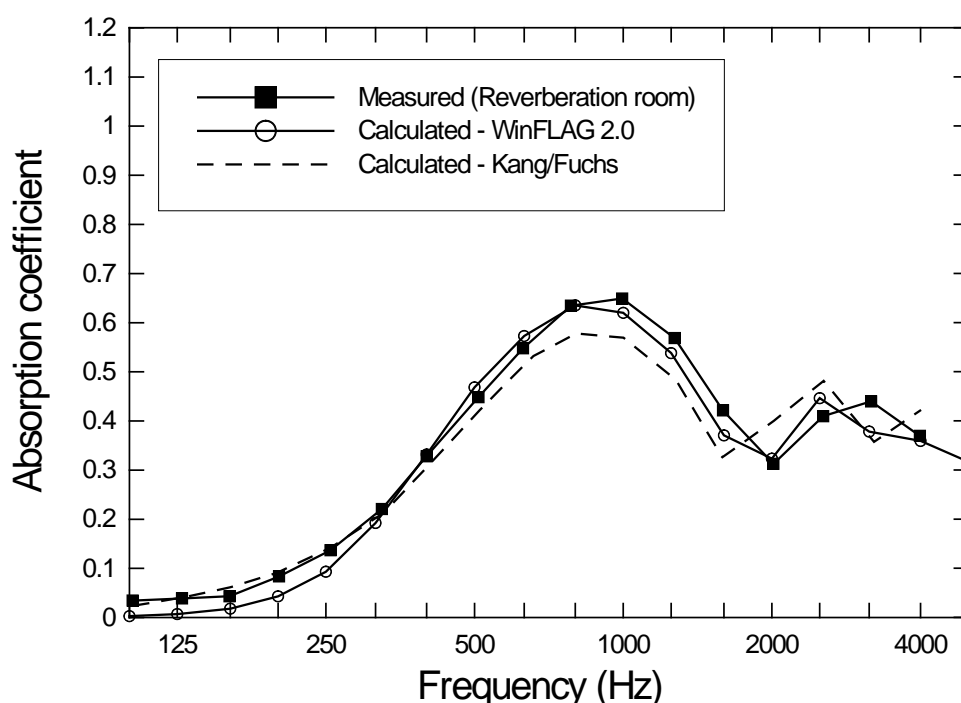


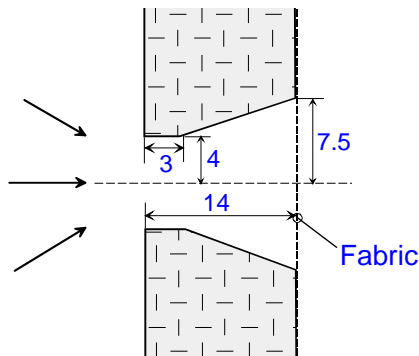
Figure C-1. Absorption coefficient for a microperforated foil (membrane) mounted against a rigid wall at a distance of 100 mm. Measurement data and calculated results by Kang & Fuchs are reproduced from figure 12 in the reference below.

Reference:

Kang, J. & Fuchs, H.V. (1999) Predicting the absorption of open weave textile and micro-perforated membranes backed by air. *J. Sound and Vibration*, **220**, 905 – 920.

ANNEX D. MEASUREMENTS AND CALCULATIONS ON A RESONATOR PANEL USING PERFORATION WITH CONICALLY SHAPED HOLES

Designing resonator absorbents using conically shaped apertures in the panels may greatly enhance the absorption capability as compared with using regular shaped holes or slits. An example is shown below; see *Figure D-2*, comparing results when using a panel with regular 8 mm diameter cylindrical holes as opposed to holes having the shape depicted in *Figure D-1*. As seen the shape has not the ideal conical shape as shown in *Figure 5-11* and presupposed in



the calculations. As seen from *Figure D-1*, however, the fit between measured and calculated data is quite good. The data for the regular case is calculated setting the exit diameter of the holes slightly larger than 8 mm ($\approx 0.5\%$ larger). In both cases the impedance correction is used.

Figure D-1. Holes in the panel having a conical part. The fabric has a flow resistance of 190 Pa.s/m.

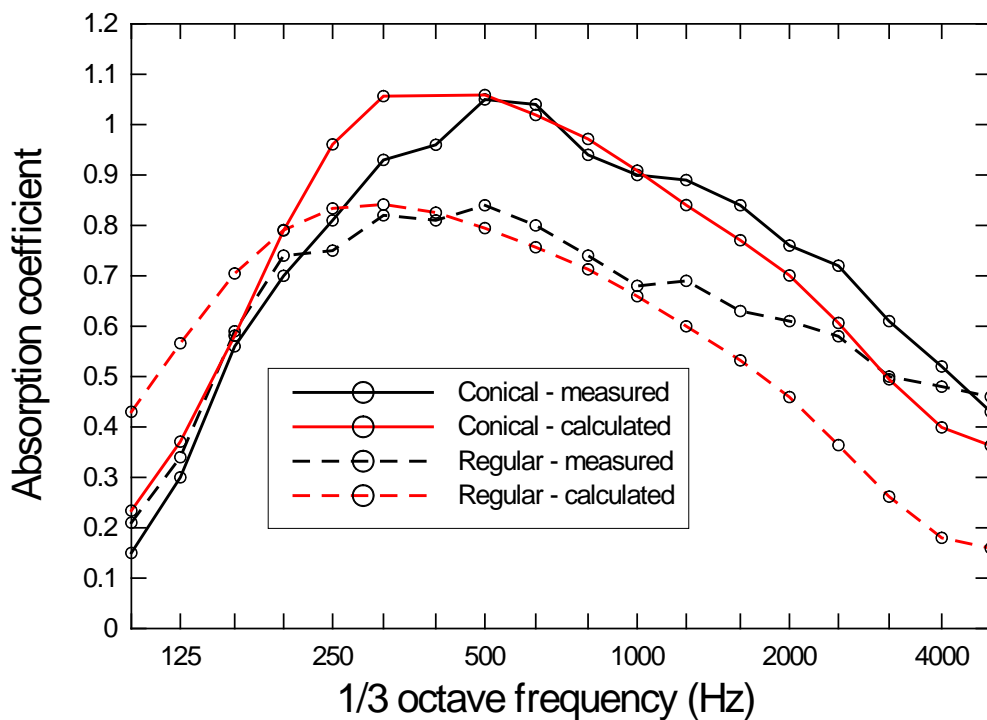


Figure D-2. Measured and calculated absorption coefficients in a reverberation room. Resonator absorbent of 14 mm perforated panel, perforation 12.5%, with a layer of fabric and mounted with airspace of 50 mm filled with mineral wool, flow resistivity 30 kPa.s/m². Measurements data taken from Figure 14 in the reference below. The shape of the conical apertures is shown in Figure D-1 above.

Reference:

Vigran, T. E. (2004) Conical apertures in panels; Sound transmission and enhanced absorption in resonator systems. *Acta Acustica united with Acustica*, **90**, 1170 – 1177.

ANNEX E. SPATIAL WINDOWING IN TRANSMISSION LOSS CALCULATIONS. EXAMPLE: THE SOUND REDUCTION INDEX OF A DOUBLE-LEAF CONSTRUCTION.

As stated in section 5.5, the main effect when applying the “spatial windowing” technique is to obtain more realistic values for the sound reduction index at low frequencies for smaller size specimen such as windows, and furthermore, greatly improving the prediction for multi-layered structures.

The measurement results shown in Figure E-1 is taken from an extensive series of measurements on double-leaf constructions performed by Hongisto et al., see reference below. Their experimental study is concentrated on the properties of the cavity, cavity absorbents and the structural connections (studs). The leaves were 2 mm thick steel plates and the area of the test opening was approximately 2.5 m².

The results shown are the data obtained for an air-filled cavity and there were no structural connections between the two steel plates. In the experiments the thickness of the cavity was varied from zero to 250 mm. Shown here are the results for a cavity thickness of 25 and 250 mm, respectively. Predicted results from NorFlag are based on the data given in the study, except for the introduction of an attenuation coefficient of 0.2 m⁻¹ (200 km⁻¹) for the air layer, this to account for unavoidable energy losses in the cavity.¹

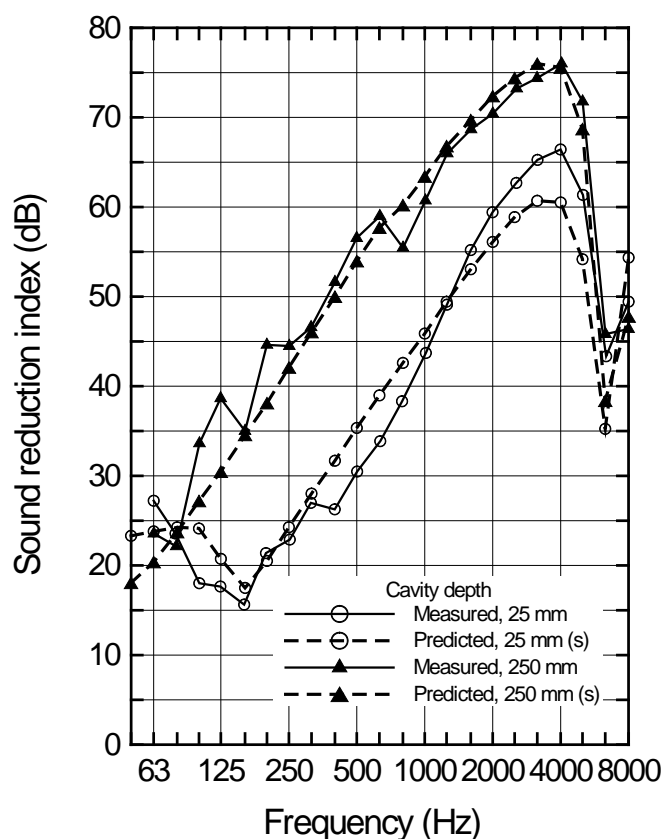


Figure E-1. Sound reduction index of a double-leaf construction of 2 mm thick steel plates with air cavity of different depth. Measured data reproduced from Figure 4a in a paper by Hongisto et al. (2002), see reference below. Predicted results from NorFlag.

References:

Hongisto, V., Lindgren, M. and Helenius, R. (2002) Sound insulation of double walls – An experimental parametric study. *Acta Acustica united with Acustica*, **88**, 904–923.

Davy, J. L. (2009) Predicting the sound insulation of walls. *Building Acoustics*, **16**, 1–20.

¹ This is equivalent to the suggestion of using a fixed absorption coefficient for wall cavities without any absorbing material, see e.g. the paper by Davy referenced above.

ANNEX F. STIFF STRUCTURAL CONNECTIONS (TIES AND STUDS) IN DOUBLE WALLS. EXAMPLE: WALL WITH ACOUSTICAL LINING.

As pointed out in section 5.2.8, the “layer” named Structural connections is strictly limited to connect plates or panels described by thin-plate theory, i.e. thin isotropic or orthotropic plates. However, experience shows that one may successfully extend the concept of “thin” to include quite thick and heavy walls. An example is shown below, comprising a 150 mm thick lightweight concrete wall of density 790 kg/m^3 with a 10 mm plaster layer with an added acoustical lining of 13 mm plasterboard. The board are mounted on studs, rigidly fastened to the wall and the cavity is filled with mineral wool, see insert sketch below. Measured and predicted results for the sound reduction index are shown in Figure F-1.

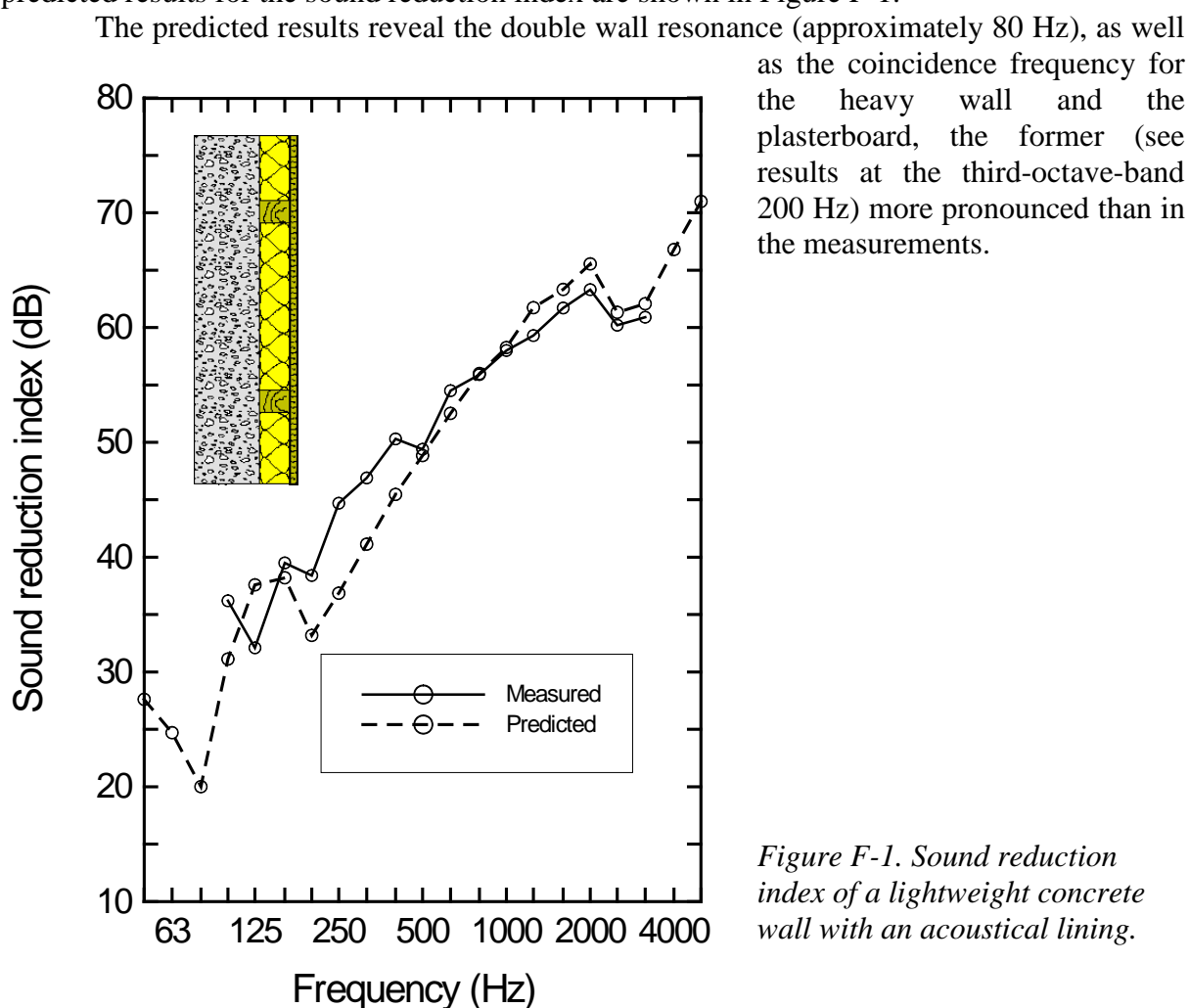


Figure F-1. Sound reduction index of a lightweight concrete wall with an acoustical lining.

ANNEX G. FLEXIBLE STRUCTURAL CONNECTIONS IN DOUBLE WALLS. EXAMPLE: LIGHTWEIGHT DOUBLE WALL WITH CAVITY INFILL

An example on the sound insulation of a double wall where stiff wooden studs connected the two leaves was presented in ANNEX F. Here an example is presented of the sound insulation of a lightweight double wall with gypsum plasterboard and mineral fibre in the cavity where flexible TC-type studs are connecting the two leaves. As pointed out in section 5.2.8.2, the equivalent stiffness (in N/m^2) of the studs is based on data from reference [2] in that section. The frequency function of this stiffness is depicted in *Figure G-1* below.

Figure G-2 shows the sound reduction index of the plasterboard double walls where the stiffness of the studs is given in *Figure G-1*. The measured data is taken from an extensive series of measurements on such walls; see reference below. In addition to the predicted result for this wall, *Figure G-2* also shows predicted results for two more cases, one for the case assuming infinitely stiff studs, the other for the no-stud case.

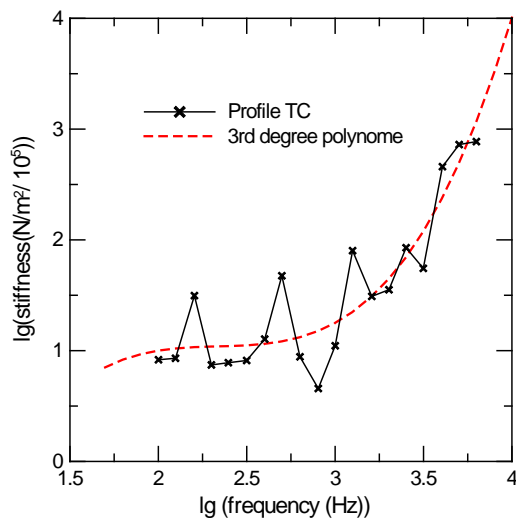


Figure G-1. Translational stiffness of C-type metal studs represented by the logarithm of the stiffness. Solid curve – data from reference [2] in section 5.2.8.2. Dashed curve – the stiffness represented by a third degree polynomial.

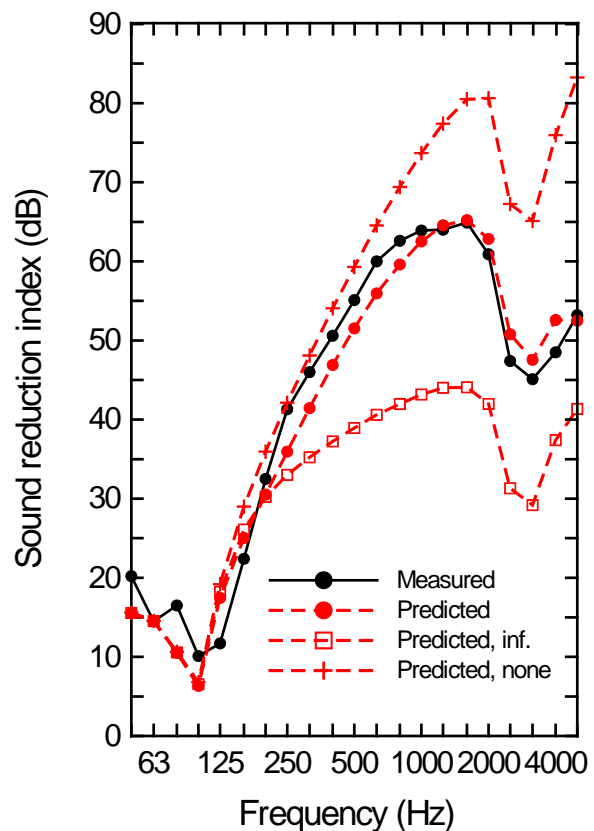


Figure G-2. Sound reduction index of lightweight double-leaf wall of 13 mm gypsum plasterboards with 65 mm cavity with mineral fiber filling. Predicted data include prediction for the wall with studs of infinite stiffness as well as the wall without studs.

R.E. Halliwell, T.R.T. Nightingale, Warnock, A.C.C. and J.A. Birta, Gypsum board walls: Transmission loss data, Internal report IRC-IR-761, Institute for Research in Construction, National Research Council of Canada, 1998.

ANNEX H1. EXAMPLE ON COMBINING SEVERAL THICK (FLEXIBLE) PLATE LAYERS. LAMINATED GLASS WITH PVB (POLYVINYL BUTYARYL)

As stated in section 5.2.7.2, the program offers the possibility to combine several elastic layers of the type denoted as thick plate. This is therefore an alternative to the sandwich layer type, which in fact is limited to three-layer combinations with identical thin face layers and a softer thicker core. The examples shown below are insulating glazing units, i.e. laminated glass constructions with viscoelastic PVB-layer, 1.52 mm thick. Approximate material properties of this type of viscoelastic layer are given by Shorter; see reference below. The elasticity modulus as well as the loss factor will be frequency dependent and also temperature dependent. However, using fixed values for the E-modulus and the loss factor, representative for the frequency range around 1000 Hz; quite good agreement with measurement data is obtained. In the example shown, the E-modulus and loss factor is set to 0.15 GPa and 0.6, respectively. Following Shorter, the Poisson ratio and density is set to 0.49 and 1000 kg/m³, respectively. The measured area of the glazing units is 2 m².

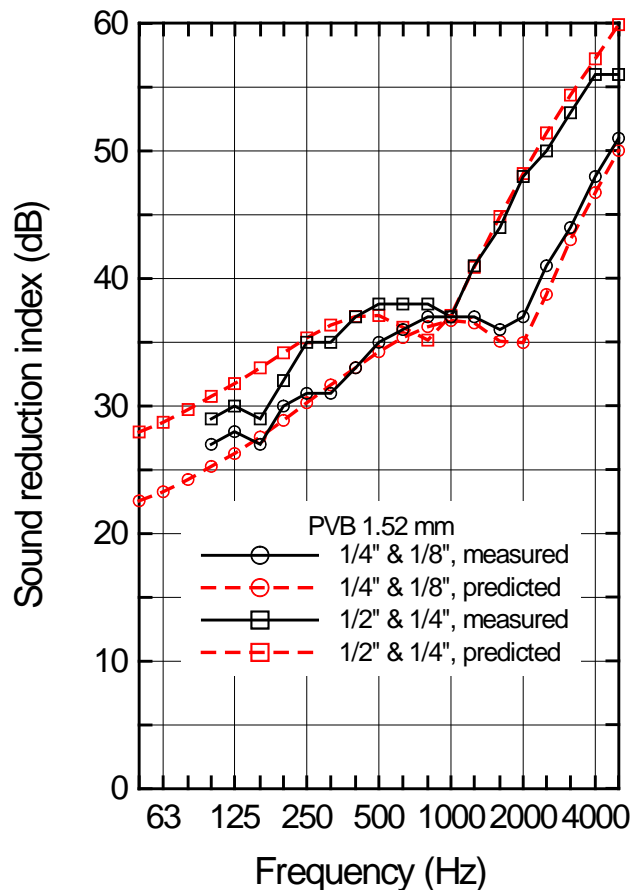
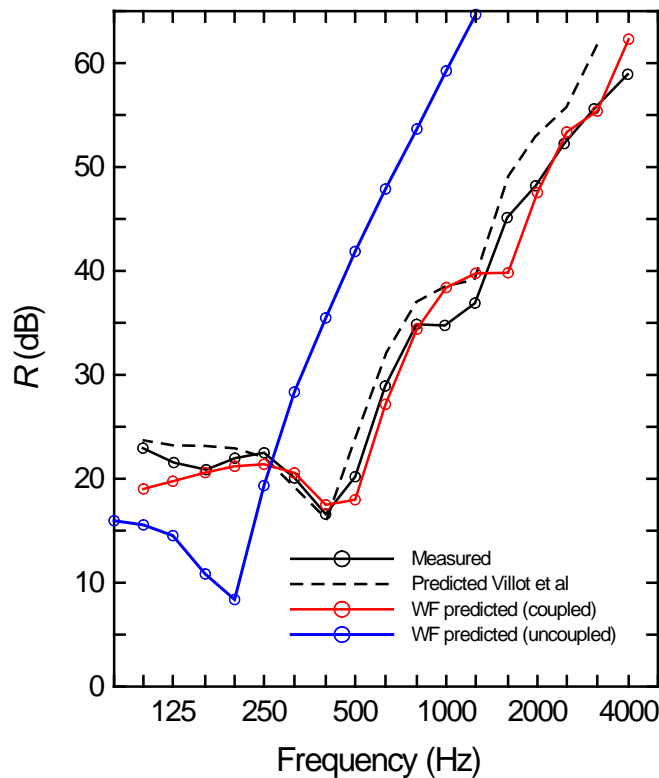


Figure H-1 Sound reduction index for two glazing units with viscoelastic 1.52 mm thick PVB-layer. The thickness (in inches) of the glasses is given in the figure legend. Measured data, courtesy Viracon, USA.

P. J. Shorter (2004) Wave propagation and damping in linear viscoelastic laminates. *J. Acoust. Soc. Am.* **115**, 1917–1925.

ANNEX H2. EXAMPLE ON COMBINING SEVERAL THICK (FLEXIBLE) PLATE LAYERS. MULTI-LAYERED PANEL; STEEL PLATE, MINERAL WOOL AND LAMINATE.

Another example on combining thick plate layers into a multilayer one is taken a paper by Villot et al., see the reference below. This multilayer construction, of area 1.3 m x 1.3 m, is composed of a 0.75 mm thick steel plate, a 30 mm dense mineral wool layer and a 3 mm thick laminate plate, all glued together. The characteristic dimensions and material data for the construction, taken from Table 2 in the given reference, are given in the table below. The



figure, showing the sound reduction index for the construction, presents four curves. The first three curves show the measured results, the predicted ones given by Villot et al. and the predicted ones using WinFlag. In the latter case the mineral wool is characterised as an elastic plate using only the first five characteristic values in the table below. As seen, the fit between measured and predicted results is quite good.

Interestingly, using the simple equivalent fluid model, denoted Allard/Johnson, for the mineral wool gives a completely different result; see the blue curve. Certainly, no stiffness is accounted for, making the layers uncoupled.

Figure H-2. Sound reduction index for a multi-layered panel; a steel plate, a mineral wool layer and a laminate plate. Measured results together with results from predictions models for the coupled case. For the uncoupled case; see description above.

	Steel	Mineral wool	Laminate
Thickness (mm)	0.75	30	3
Density (kg/m ³)	7850	90	1360
E-modulus (Gpa)	210	0.4·10 ⁻³	0.6
Poissons number	0.3	0	0.15
Loss factor	0.03	0.018	0.015
Flow resistivity (kPa.s/m ²)		34	
Tortuosity		1	
Porosity		0.955	
Viscous length (μm)		40	
Thermal length (μm)		80	

Reference:

M.Villot, C. Guigou and L. Gagliardini (2001) Predicting the acoustical radiation of finite size multi-layered structures by applying spatial windowing of infinite structures.

J. Sound & Vibration **245**, 433–455.

ANNEX I. EXAMPLE ON DOUBLE POROSITY MATERIAL. MEASURED AND PREDICTED RESULTS ON A FIBROUS MATERIAL.

In Section 5.2.3.6 an example was given on the effect of meso-perforations on the absorption coefficient of the porous material, using a set of default-data and comparing with the results of the non-perforated material.

Below is shown an example of the absorption coefficient of such a double porosity material, a measured result compared with predicted results using a FEM-model and also the model implemented in WinFlag (now NorFlag), both models assuming a rigid skeleton for this fibrous material. The measured result and the predicted one using FEM are reproduced from Figure 7 in the referenced paper below, which also treat the non-rigid cases. However, in this case of a heavy fibrous material, see the table of material properties below, the differences are very small. As seen from the figure, the model by Sgard et al.; see Section 5.2.3.6, implemented in WinFlag gives a good fit to the measured ones in the lower frequency range where the effect of the perforations is important but underestimates somewhat in the higher frequency range.

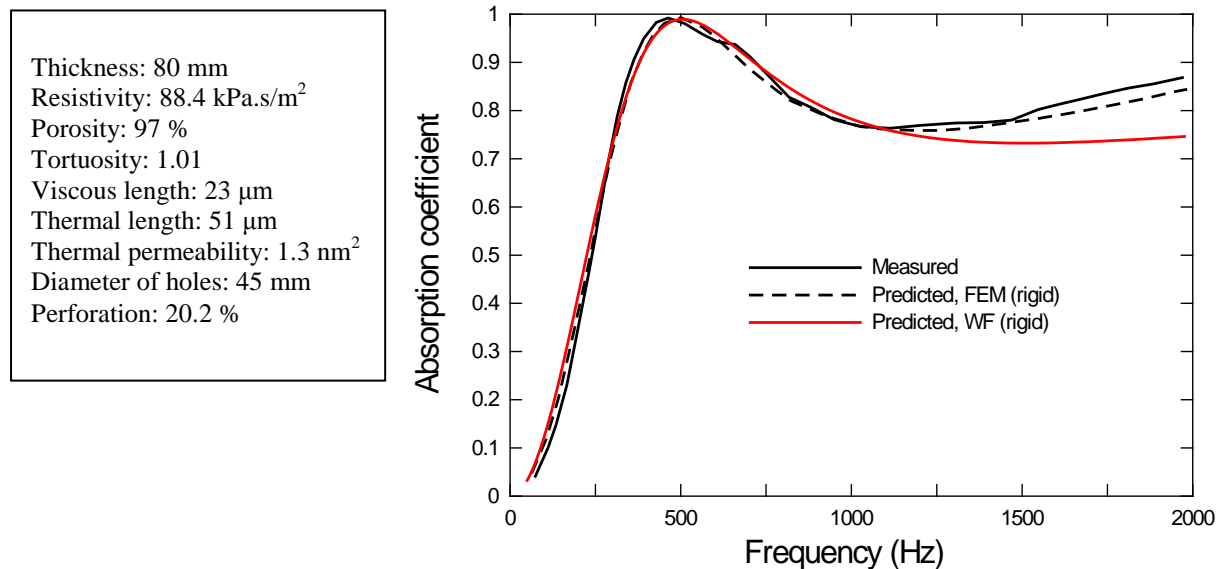


Figure I 1. Measured and predicted absorption coefficient at normal incidence for a double porosity fibrous material with the material properties given in the table. Data partly reproduced from Figure 7 in the paper by Bécot et.al, see reference below.

Reference:

F.-X. Bécot, O. Dazel and L. Jaouen. Structural effects in double porosity materials: analytical modelling and numerical validation. ISMA 2010, Leuven, Belgium.